NACA RM L52D01

NACA

RESEARCH MEMORANDUM

A STUDY OF THE FLOW OVER A 45° SWEPTBACK WING-FUSELAGE COMBINATION AT TRANSONIC MACH NUMBERS

By Richard T. Whitcomb and Thomas C. Kelly

Langley Aeronautical Laboratory
Langley Field, Va.

NATIONAL ADVISORY COMMITTEE
FOR AERONAUTICS

WASHINGTON
June 25, 1952

NATIONAL ADVISORY COMMITTEE FOR AERONAUTICS

RESEARCH MEMORANDUM

A STUDY OF THE FLOW OVER A 45° SWEPTBACK WING-FUSELAGE COMBINATION AT TRANSONIC MACH NUMBERS

By Richard T. Whitcomb and Thomas C. Kelly

SUMMARY

Pressure distributions, tuft patterns, and schlieren surveys have been obtained for a sweptback wing-fuselage combination in the Langley 8-foot transonic tunnel at Mach numbers to 1.11 and angles of attack to 20°. The wing had 45° of sweepback, an aspect ratio of 4.0, a taper ratio of 0.6, and an NACA 65A006 airfoil section. A study of the results of these measurements indicates the development of various phenomena with increases in Mach number and angle of attack. Among these phenomena are the development of the shock on the wing, the initiation and rearward movement of a strong normal shock behind the trailing edge of the wing-fuselage juncture, the onset of the bow shock ahead of the wing leading edge, and the increase and reduction of the boundary-layer separation and the leading-edge boundary-layer vortex.

INTRODUCTION

Several detailed wind-tunnel investigations (refs. 1 and 2, for example) have provided a basis for the understanding of the flow over sweptback wings at high-subsonic Mach numbers. On the basis of these data and pressure data obtained from the wing-flow method (ref. 3) the nature of the flow over sweptback wings at transonic speeds has been conjectured. Because of the previous speed limitations of wind tunnels, however, it has been impossible to obtain a more detailed investigation of the nature of this flow at transonic speeds. A slotted test section which allows an investigation of relatively large models in the transonic range to a Mach number of 1.14 recently has been installed in the Langley 8-foot transonic tunnel. With this new facility, a detailed investigation of the flow phenomena over a 45° swept-wing - fuselage combination has been made. The results of this study provide not only a contribution to the knowledge of the flow over swept wings in the transonic range but also an indication of the nature of sweptback wing-fuselage interference at transonic Mach numbers.

The data to be discussed include pressure distributions, tuft patterns, and schlieren surveys. Through consideration of these data it has been possible to present a qualitative description of development of shock waves and boundary-layer separation on the wing and fuselage at transonic Mach numbers.

APPARATUS

The Langley 8-foot transonic tunnel is a single-return, dodecagonal, slotted-throat wind tunnel which operates at a stagnation pressure approximately equal to atmospheric pressure. The tunnel is capable of continuous operation up to a Mach number of 1.14. A complete description of the Langley 8-foot transonic tunnel may be found in reference 4.

The model configuration for the present investigation had a wing with 45° sweepback of the quarter-chord line, an aspect ratio of 4, a taper ratio of 0.6, and an NACA 65A006 airfoil section parallel to the air stream. The fuselage of the combination, which is shown in figures 1 and 2, had a fineness ratio of 10 based on model diameter and length from the model nose to intersection with the sting. Two models were used to obtain these data. One, used for pressure measurements, had a wing constructed of a mild steel core with a tin-bismuth-alloy covering and is described in reference 5; the other, used for schlieren surveys, tuft surveys, and force measurements, had a wing constructed of 14S-T aluminum alloy and is described in reference 6. The model used for pressure measurements is shown mounted in the 8-foot slotted test section in figure 1. General dimensions of the models and locations of pressure orifices on the wing and fuselage are presented in figure 2.

Tuft surveys were made with alternate rows of nylon line and wool yarn cemented directly to the surface of the model. The very flexible wool-yarn tufts gave a good indication of slight changes in flow direction. The less flexible thin nylon tufts remained on the wing longer at higher Mach numbers, however, and gave a good indication of violent separation. It was found also that the difference in the thicknesses of the two types of tufts could be used to determine the relative thickness of the boundary layer. Schlieren photographs were made with the temporary single-pass system described in reference 4.

RESULTS

The data to be analyzed are presented as individual groups for given survey conditions. Each group consists of pressure data, force data, tuft

patterns, and schlieren surveys. Survey conditions for various Mach numbers at each of several angles of attack are presented in figures 3 to 8.

Pressure data to be analyzed are presented in the form of pressure-coefficient profiles plotted at the five semispan measurement stations on a plan form of the wing and at six radial locations on an outline of the fuselage. The pressure coefficient P is defined as $\frac{p_l - p_0}{q_0}$ where p_0 and q_0 are the free-stream static and dynamic pressures, respectively, and p_l is the local static pressure. The pressure data were taken directly from the tabulated data of references 5 and 7. Force data and tuft-pattern photographs are presented with each pressure-coefficient profile. Variations of the force results with Mach number are presented in figure 9. Force and tuft data were taken from more complete unpublished data obtained in the Langley 8-foot transonic tunnel.

Schlieren data are presented for most cases in the form of composite side views and plan views of the model. The plan-view composite is placed at the correct spanwise location for 0° angle of attack. The axial locations of the wing root and tip are also shown in the schlieren side view. Photographs used to construct the composite side view were obtained by using a stationary schlieren system and moving the model both longitudinally and vertically in the test section. The plan views were obtained by rotating the model 90° and offsetting it vertically. Because the individual pictures used in the schlieren composites were taken during separate runs, slight variations in the tunnel Mach number result in discontinuities of the various shocks as they extend from one picture of the composite to another. The grid lines shown in most of the schlieren photographs are approximately parallel and normal to the flow. The object shown above the rearward end of the fuselage for the 4° angle-of-attack case is a probe which was used to measure fluctuations in downwash angle. The probe had no noticeable effect on the schlieren indications. It should be noted that the scale of the schlieren composites and that of the pressure profiles are not equal.

DISCUSSION

For convenience, the discussion is divided into considerations of the phenomena at individual angles of attack and Mach numbers. Throughout these individual discussions, however, the development of various phenomena with increases in Mach number and angle of attack will be noted. Among these phenomena are the expansion of the field of flow of the body, the development of the shock on the wing, the initiation and rearward

movement of a strong normal shock behind the trailing edge of the wing-fuselage juncture, the onset of bow shock ahead of the wing leading edge, and the increase and reduction of the boundary-layer separation and the leading-edge boundary-layer vortex.

Angle of Attack of 0°

At an angle of attack of 0° and a Mach number of 0.85 (fig. 3(a)) the pressure distributions and tuft surveys indicate the presence of typical subcritical flow on the wing and fuselage. The drag is similar to that at other subsonic Mach numbers and disturbances in the field about the model are slight, as indicated by the schlieren photographs. The pressure data of reference 5 for the fuselage-alone configuration indicate that the increase in the velocity on the fuselage due to the presence of the fuselage is of the order of 0.03 in Mach number at a Mach number of 0.85. The extent of this region of induced velocities is relatively local, and therefore, for the wing-fuselage configuration, only the inboard sections of the wing would be significantly affected.

For a Mach number of 0.90 (fig. 3(b)) supercritical conditions exist over most of the wing semispan and on the fuselage in the region of the wing-fuselage juncture. It should be noted, however, that based on the component of velocity normal to wing leading edge the flow over the wing is still subcritical. The schlieren composite indicates the presence of weak shock waves in the region above the wing-fuselage juncture. Comparison of this picture with those obtained at other times indicates that these shocks are extremely transitory in nature. There is no perceptible drag rise associated with the formation of these shocks.

At a Mach number of 0.94 (fig. 3(c)), a stronger, extensive shock stabilizes at the trailing edge of the wing-fuselage juncture as shown in the schlieren composite. The presence of the shock is indicated by the dark, shaded region at (a) in figure 3(c). This shock is approximately normal to the wing surface and, as evidenced by the pressure distributions, extends laterally normal to the plane of symmetry to beyond the 60-percent-semispan station. The pressures measured on the fuselage indicate that the shock emanating from the wing-fuselage juncture trailing edge extends with nearly uniform strength around the fuselage. The nearly normal shock crossing the wing tip ((b) in fig. 3(c)) is associated with disturbances produced by the tip. The other weak shocks are transitory. Tuft patterns show no changes in the boundary layer on the wing or fuselage. The force results indicate that a slight increase in drag coefficient is associated with the development of the shock on the wing at this Mach number.

The pressure distributions on the fuselage and side-view schlieren pictures of figure 3(d) indicate that, when the Mach number is increased to 0.97 the shock originating at the trailing edge of the wing-fuselage juncture ((a) in fig. 3(d)) becomes relatively weak and slopes rearward. These same data indicate a strong, nearly normal shock (b) develops approximately one-half chord length behind the wing-fuselage juncture. The shading downstream of the strongest indication of this shock (b) indicates that it curves rearward from the plane of symmetry. Although the shock (a) is not sufficiently strong to be visible in the lowest side-view schlieren picture, it probably extends outward to merge with the shock (b) at approximately (c). The pressure distributions on the wing indicate that the shock (b) crosses the rearward portion of the wing and merges with shock (a) in the midsemispan region. The shock resulting from the merger crosses the outboard region of the wing and extends nearly normal to the stream well beyond the wing tip, as indicated by the schlieren plan view at (d). The portions of the shock beyond the wing tips which are nearly normal to the stream are also visible in the side view at (d). The shading forward of the strongest indications of the shock (d) in the side view are further indications of the forward extension of the shock ahead of the normal portions as shown directly in the plan view. The two dark regions (e) visible in the plan-view schlieren at a Mach number of 0.97 behind the wing-fuselage-juncture trailing edge are associated with the nearly normal portions of the combined shock shown at (e) in the lower side-view picture. This relationship is indicated by the shadings ahead of the darkest regions and the dual nature of the indications. The fact that these indications (e) in the plan view are not at the same streamwise station as the normal region at (e) in the side view is due to slight differences in the test Mach numbers for the two pictures. The double indications are associated with a slight angle of attack of the model with respect to the stream. The angle of these dark regions (e) with respect to the stream direction indicates that at a vertical distance from the combination the shock is nearly normal to the stream in the spanwise as well as the vertical direction. This phenomenon results from the rearward slope of the shock near the plane of symmetry and the forward slope near the tip, as shown in the side view.

The waves (f) which appear above and below the juncture in the schlieren composite were caused by $\frac{1}{2}$-inch long, 0.02-inch-diameter wire segments placed normal to the air stream on the upper and lower surfaces of the fuselage. It has been shown (ref. 4, for example) that small disturbances in the flow generate waves which cross the flow at approximately the Mach angle and yet can be detected by schlieren apparatus. It was hoped, therefore, that the protuberances on the fuselage would provide an indication of the Mach number distribution in the region of the wing-fuselage juncture. The protuberances were sufficiently large, however, to produce a strong complex field to points

at least one diameter from the fuselage surface, and indications of the Mach number distribution provided by the angles of the waves are inaccurate in that region. Waves emanating from the protuberances become somewhat weaker several diameters from the fuselage surface and do provide a fairly reliable indication of the Mach number variation at a distance from the fuselage. The extent of the waves (fig. 3(d)) indicates the presence of supersonic velocities well above the fuselage surface for this stream Mach number of 0.97. A measurement of the wave angle at a point approximately three diameters above the juncture trailing edge indicated a Mach number of 1.02 in that region.

The pressure data of reference 4 indicate that at this Mach number of 0.97 the induced Mach number increment on the surface of the fuselage alone is approximately 0.04. Schlieren photographs obtained at this condition show that the increased velocity field extends well into the stream and for the wing-fuselage combination the entire forward portion of the wing is operating in a Mach number field considerably higher than the stream value. Also the pressures on the forward portion of the wing are generally considerably more negative than those for a wing alone. The pressure distributions and schlieren surveys for the fuselage alone (ref. 4) indicate that no shock is present on the fuselage alone at this Mach number; thus, the strong normal shock (b) behind the trailing edge of the wing-fuselage juncture of the combination must be associated with the wing. The strength of this shock for the wing in the presence of fuselage, however, is probably somewhat greater than it would be for a wing alone.

At a Mach number of 0.99 (fig. 3(e)) the oblique shock originating at the trailing edge of the wing-fuselage juncture (a) is still relatively weak at the plane of symmetry. At stations farther outboard on the semispan, the Mach number ahead of the shock and the pressure change through the shock are greater than those for the inboard region and thus indicate that this shock is probably somewhat stronger on the outboard region. When the Mach number is increased to 0.99, the strong, nearly normal shock present behind the trailing edge of the wing-fuselage juncture at the lower Mach number of 0.97 moves downstream to a position opposite the tip of the wing ((b) in fig. 3(e)). This shock extends vertically from the fuselage in a direction nearly normal to the stream. In the plane of the wing it extends nearly normal to the stream from the fuselage surface but at a short distance from the fuselage it turns forward, as shown in the plan view at (c). Because of this forward movement, the shock (b) crosses the rearward region of the outboard portion of the wing and leaves the tip at (d). The forward movements of the shock (b) onto the wing tips are also shown in the side view at (c). Just outboard of the wing tip the weak shock originating at the wing-fuselage juncture (a) merges with the strong normal shock (d). The combined shock (e) extends toward the tunnel wall at a moderate angle with respect to the stream. At short distances above and below the wing plane the

shock (b) turns rearward slightly in the lateral direction, as shown by the shading at (f) in the side and plan views.

The combined shock for the model at a Mach number of 0.99 strikes the tunnel walls at (g) in figure 3(e). The discontinuity in the indications of this contact in the plan-view pictures is due to a slight difference in the Mach numbers for the two pictures. The incidence of the shock on the wall indicates that the flow field of the model has expanded sufficiently to produce supersonic velocities at the tunnel wall. The wall pressures indicate a maximum Mach number increment of 0.02 was produced by the model at the wall at near-sonic Mach numbers (ref. 4).

Since a normal shock is present on the fuselage alone at a Mach number of 0.99 (ref. 4) at the same location as the normal shock (b) on the fuselage combination, it may be assumed that this shock on the combination is due in part to the fuselage. The induced velocities ahead of the shock on the combination, however, are somewhat higher than those on the fuselage alone because of the expanded field of the outboard regions of the wing. The shock on the fuselage of the combination, therefore, is probably stronger than that on the fuselage alone. On the basis of the pressures measured on the fuselage of the combination and the shock patterns observed at the lower Mach number of 0.97, it may be expected that a normal shock similar to that emanating from the fuselage would be present behind a wing alone and would probably stand somewhat forward of its location on the combination.

The schlieren composite shows a bow wave, associated with the deceleration of the local supersonic flow induced by the fuselage, located about one-half-chord length forward of the wing-fuselage-juncture leading edge ((h) in fig. 3(e)). Force coefficients indicate a rather abrupt drag rise for the combination when the Mach number is increased from 0.94 to 0.99. Since the tufts show only slight changes in the boundary layer, most of the drag increase is probably due to the development of strong shocks rather than to separation. For thicker wings and those with less sweep, the drag increase at high subsonic Mach numbers is due primarily to separation (ref. 1).

Schlieren photographs obtained at a Mach number of 1.00, but not presented, indicate that, when the Mach number is increased from 0.99 to 1.00, the strong, nearly normal shock originating from the surface of the fuselage moves downstream and no longer crosses the tip of the wing as it does at a Mach number of 0.99. With a further increase in Mach number to 1.02, this shock continues to move downstream and reaches the positions shown at (b) in figure 3(f). A comparison of the data presented for the combination with that for the fuselage alone (ref. 4) indicates that this shock is farther rearward when the wing is present. The change in the pressure distribution on the fuselage associated with

this movement results in a significant increase in the pressure drag for the fuselage. Thus, although the shock on the fuselage of the combination appears of the same strength as that on the fuselage alone, the losses associated with it must be greater. The shock (a) originating at the trailing edge of the wing-fuselage juncture is still relatively weak at this Mach number. The most outboard pressure distribution on the wing indicates an increase in pressure near the trailing edge which is apparently not associated directly with the shock (a) crossing the wing semispan. This pressure change is associated with disturbances originating at the tip. The effect of these disturbances on the field is shown at (c) in the schlieren side and plan views of figure 3(f). The various disturbances emanating spanwise from the tip merge at a short distance from the tip to form a relatively strong shock at (d). This shock (d) associated with the wing apparently merges with that at (b) produced primarily by the fuselage several semispans outside the schlieren view. The bow shock associated with the wing is shown at (e) in figure 3(f). The second disturbance which appears in the schlieren composite in the region above the wing-fuselage juncture (f) is the intersection of the bow shock (e) on the tunnel wall. At the lower Mach number of 0.99 this shock does not extend to the wall.

With an increase in Mach number to 1.11 (fig. 3(g)), the shock originating at the trailing edge of the wing-fuselage juncture (a) is swept nearly to the tip trailing edge. The secondary disturbances associated with the tip at a Mach number of 1.02 (fig. 3(f)) disappear at this higher Mach number of 1.11. The bow shock (c) is apparently attached to the leading edge of the juncture. The shock (b) associated with the fuselage of the combination moves off the surface of the fuselage as it does for the fuselage alone (ref. 4). The pressure distributions on the rearward end of the fuselage are the same as those on the fuselage alone. No separation is indicated by the tuft patterns at this Mach number as at lower Mach numbers. At higher Mach numbers the shock originating at the wing-fuselage-juncture trailing edge would move further rearward on the wing and finally to the trailing edge where it would remain at all higher Mach numbers. The root bow wave would become more inclined and would reach the leading edge of the wing at a Mach number of approximately 1.40.

Angle of Attack of 4°

At an angle of attack of 4° and a Mach number of 0.85 (fig. 4(a)) the pressure distributions indicate supercritical flow over the forward portions of the upper surface of the wing. Relatively high Mach numbers are associated with the negative pressure peaks formed at the upper-surface leading edge, a value of 1.62 being indicated at the 80-percent-semispan station. No apparent drag rise is associated with the supercritical conditions. The schlieren composite indicates weak shocks

associated with the supercritical velocities in the region above the wing-fuselage juncture. The weak shock waves shown above the wing tip are probably caused by disturbances acting parallel to the stream in the near-sonic velocity field adjacent to the tip. These waves are possibly associated with the weak separation near the tip.

At a Mach number of 0.90 (fig. 4(b)), a shock, which appears to originate at the wing-fuselage-juncture trailing edge and which is approximately normal to both the wing surface and the plane of symmetry, is indicated by the schlieren composite ((a) in fig. 4(b)) and the pressure distributions. This shock is similar in appearance to one which occurred on the wing at an angle of attack of 0° and a Mach number of 0.94. Several disturbances, which seem to emanate from the lower surface of the fuselage in the schlieren composite (b), are associated with the near-sonic flow indicated on the lower surfaces of the wing and fuselage by the pressure distributions. A disturbance approximately normal to the flow located just back of the tip and extending laterally well beyond the tip is shown in the schlieren plan-form view at (c). This disturbance may be associated with the deceleration of a wide accelerated flow field around the wing-fuselage combination. It is similar in nature to that for a body alone. (See fig. 4(g).)

A definite drag rise occurs when the Mach number is increased to 0.94. The noticeable redirection of the tufts outward on the rear portions of the upper surface of the wing behind the shock which originates at the wing-fuselage-juncture trailing edge indicates a thickening of the boundary layer at this condition which may be associated with limited separation. It would appear, therefore, that the drag rise for this condition is due in part to additional boundary-layer losses as well as to shock losses, unlike the case at an angle of attack of 0° where the drag rise was due almost entirely to shock losses. The shock (a) extending above the trailing edge of the wing-fuselage juncture in the side-view schlieren composite for a Mach number of 0.94 (fig. 4(c)) is considerably stronger than that for an angle of attack of 0°, as might be expected. Conversely, the shock (b) below the juncture is weaker than for 0°. The pressures and schlieren surveys indicate that near the tips the shock above the wing is much stronger and more extensive for 4° than for an angle of attack of 0° (see (c) in fig. 4(c)). The indications of the shocks above the two tips vary considerably in intensity and extent. Photographs taken at other instants for this same condition indicate that the differences between the strengths of the shock on the two wing tips is due to unsymmetrical fluctuations of the disturbances since at some instants the shock is more nearly equal in strength on the two tips. Although it is not perceptible in the composite schlieren photograph, pressure distributions indicate the presence of an oblique shock associated with the leading-edge peaks. The pressure distributions indicate that this oblique shock merges with the juncture trailing-edge shock in the vicinity of the tip.

At Mach numbers of 0.97, 0.99, and 1.02 (figs. 4(d) to 4(f)) the general nature of the shock formation above the wing-body combination for an angle of attack of 4° is similar to that for 0° at the same Mach numbers, although the magnitudes and positions of the shocks differ. The weak oblique shock which apparently emanates from the tip leading edge at a Mach number of 0.99 ((a) in fig. 4(e)) is probably associated with the initiation of a tip vortex. The relatively weak oblique shock (a) ahead of the main fuselage shock (b) at a Mach number of 1.02 (fig. 4(f)) and the complex shock formation (a) above the fuselage at a Mach number of 1.11 (fig. 4(g)) are associated with the flow over the fuselage at an angle of attack.

Tuft surveys (fig. 4(f)) show that the shock originating at the wing-fuselage-juncture trailing edge still leads to a thickening of the boundary layer at a Mach number of 1.11 although the extent of the thickened boundary layer is less than at lower Mach numbers when the juncture shock was farther forward on the wing.

Angle of Attack of 6°

At an angle of attack of 6° and a Mach number of 0.80 (fig. 5), the regions of negative pressure on the upper surface of the sections near the leading edge become progressively broader from the root to the tip and suggest the presence of a separation vortex such as that described in reference 8; the fine nylon tufts are directed outward in the regions of high negative pressures so that the presence of a leading-edge separation vortex is again suggested. The heavier yarn tufts, which extend further into the stream from the model surface, are not directed outward as much as the fine woven tufts and indicate that the region of reversed flow of the vortex is quite thin. At the tip sections the relatively low level of negative pressures on the upper surface, the relatively poor pressure recovery at the trailing edge, and the slight outward direction of the tufts are indicative of a thickened boundary layer over the entire chord.

Angle of Attack of 8°

With an increase in angle of attack to 8° at a Mach number of 0.80 (fig. 6(a)), the pressure distributions and tuft surveys indicate a marked rearward spread and a considerable strengthening of the leading-edge separation vortex. Complete separation over the wing from a station just inboard of the 80-percent-semispan station out to the tip is indicated by pressure surveys.

With an increase in Mach number to 0.85 (fig. 6(b)), tuft patterns show that outward flow in the boundary layer on the leading edge of most

of the semispan and over the entire chord on sections inboard of the 50-percent-semispan station has disappeared; this condition indicates that the leading-edge separation vortex has been eliminated in these regions. The vortex type of flow has been replaced by an attached supersonic accelerating flow around the leading edge of the type described in reference 9.

When the Mach number is increased through 0.90 to 0.99 the extent of the vortex and separation contract outboard and rearward (figs. 6(c) and 6(d)). The tuft patterns and pressure distributions indicate that, at a Mach number of 0.99, the extent of severe boundary-layer losses on the wing upper surface is limited to the region back of the adverse gradients, associated with the shock. At this condition, the flow phenomena are similar in nature although different in magnitude to the flow phenomena which existed at a corresponding Mach number and an angle of attack of 4°.

With an increase in Mach number to 1.11 (fig. 6(e)) the shock which originates at the wing-fuselage-juncture trailing edge moves farther rearward as it crosses the wing as it did at lower angles of attack. The pressure distributions indicate that this shock causes a distinct pressure discontinuity as it crosses the tip section. There is a possibility that the boundary layer is extremely thin over this region of the tip so that the field pressure disturbance is allowed to extend nearly undistorted to the model surface.

Angle of Attack of 12°

As the angle of attack is increased to 12° at a Mach number of 0.80 (fig. 7(a)) the leading-edge separation vortex spreads rapidly rearward with complete separation over the wing evident from the 30-percent-semispan station out to the tip.

With increases in Mach number to 0.89 (fig. 7(b)), 0.99 (fig. 7(c)), and 1.11 (fig. 7(d)), the separated region on the upper surface of the wing contracts outward and rearward as it did at lower angles of attack. At a Mach number of 1.11, separation is confined to the region back of the adverse pressure gradients on the midsemispan and outboard sections. Because of the reattachment of the boundary layer, the lift carried by the outboard regions of the wing increases as the Mach number is raised from 0.89 to 0.99 and, as a result, the lift of the entire wing increases. With a further rise in Mach number to 1.11, the lift on outboard sections continues to increase, while on the inboard sections a decrease in lift is noted, because of the presence of a supersonic type of flow over these regions.

Angle of Attack of 20°

At an angle of attack of 20° and at Mach numbers of 0.79 (fig. 8(a)) and 0.89 (fig. 8(b)) severe separation of the flow over the entire upper surface of the wing is indicated by the tuft patterns. Because of the complete separation, the negative pressures on each of the sections are very nearly uniform with the negative pressure level decreasing from root to tip and indicate more severe separation on the outboard sections. The greater severity of separation on the outboard sections is also shown by the tuft patterns. As the Mach number is increased to 0.99 (fig. 8(c)), the pressure distributions and tuft patterns indicate a reattachment of the flow on the rear portions of the sections near the root. With a further increase in Mach number to 1.11 (fig. 8(d)), this region of flow reattachment spreads slightly outward.

At a Mach number of 1.11, the absolute pressures on the inboard upper surface of the wing approach absolute zero, the limiting pressure coefficient at this Mach number being about -1.16.

CONCLUDING REMARKS

A study of the pressure distributions, tuft patterns, and schlieren surveys obtained for a 45° sweptback wing-fuselage combination forms the basis for the following general remarks.

At angles of attack of 0° and 4° a strong normal shock develops behind the trailing edge of the wing-fuselage juncture at a Mach number of 0.97. This shock crosses the wing at Mach numbers of 0.97 and 0.99. At higher Mach numbers it moves downstream of the wing.

A shock, which originates at the trailing edge of the wing-fuselage juncture, develops at a Mach number of 0.94. This shock slopes rearward and becomes relatively weak as the Mach number is increased to 1.00. This shock merges with the strong normal shock behind the wing juncture and the combined shock extends well beyond the wing-fuselage combination at near-sonic Mach numbers.

Because of the induced flow over the fuselage, a bow shock forms somewhat forward of the wing-root leading edge at a Mach number of 0.99. This shock moves rearward with increasing Mach number and is at the root leading edge at a Mach number of 1.11.

Tuft patterns and pressure distributions indicate no separation over the wing for all test Mach numbers at an angle of attack of 0°. At an angle of attack of 4° increased boundary-layer losses form between Mach numbers of 0.89 and 0.94 on the midsemispan and outboard sections

of the wing back of the shock originating at the wing-fuselage-juncture trailing edge. With further increases in Mach number, the region of increased boundary-layer losses contracts rearward.

At an angle of attack of 8° and a Mach number of 0.80, the tuft patterns indicate the presence of a leading-edge separation vortex and separation over the midsemispan and outboard sections of the wing. As the Mach number is increased to transonic values, the flow reattaches over the forward regions of the wing. At Mach numbers higher than 0.99 separation is confined to the region back of the shock which originates at the wing-fuselage-juncture trailing edge.

At an angle of attack of 20° and a Mach number of 0.79 the flow is separated over the entire upper surface of the wing. At Mach numbers of 0.99 and higher, the tuft patterns indicate a reattachment of the flow on the rearward regions of the inboard sections.

Langley Aeronautical Laboratory
National Advisory Committee for Aeronautics
Langley Field, Va.

REFERENCES

1. Whitcomb, Richard T.: An Experimental Study at Moderate and High Subsonic Speeds of the Flow Over Wings With 30° and 45° of Sweepback in Conjunction With a Fuselage. NACA RM L50K27, 1951.

2. Edwards, George G., and Boltz, Frederick W.: An Analysis of the Forces and Pressure Distribution on a Wing With the Leading Edge Swept Back 37.25°. NACA RM A9K01, 1950.

3. Danforth, Edward C. B., and O'Bryan, Thomas C.: Pressure-Distribution Measurements Over a 45° Sweptback Wing at Transonic Speeds by the NACA Wing-Flow Method. NACA RM L51D24, 1951.

4. Ritchie, Virgil S., and Pearson, Albin O.: Calibration of the Slotted Test Section of the Langley 8-Foot Transonic Tunnel and Preliminary Experimental Investigation of Boundary-Reflected Disturbances. NACA RM L51K14, 1952.

5. Loving, Donald L., and Estabrooks, Bruce B.: Transonic-Wing Investigation in the Langley 8-Foot High-Speed Tunnel at High Subsonic Mach Numbers and at a Mach Number of 1.2. Analysis of Pressure Distribution of Wing-Fuselage Configuration Having a Wing of 45° Sweepback, Aspect Ratio 4, Taper Ratio 0.6, and NACA 65A006 Airfoil Section. NACA RM L51F07, 1951.

6. Osborne, Robert S.: A Transonic-Wing Investigation in the Langley 8-Foot High-Speed Tunnel at High Subsonic Mach Numbers and at a Mach Number of 1.2. Wing-Fuselage Configuration Having a Wing of 45° Sweepback, Aspect Ratio 4, Taper Ratio 0.6, and NACA 65A006 Airfoil Section. NACA RM L50H08, 1950.

7. Loving, Donald L., and Williams, Claude V.: Basic Pressure Measurements on a Fuselage and a 45° Sweptback Wing-Fuselage Combination at Transonic Speeds in the Slotted Test Section of the Langley 8-Foot High-Speed Tunnel. NACA RM L51F05, 1951.

8. Lange, Roy H., Whittle, Edward F., Jr., and Fink, Marvin P.: Investigation at Large Scale of the Pressure Distribution and Flow Phenomena Over a Wing With the Leading Edge Swept Back 47.5° Having Circular-Arc Airfoil Sections and Equipped With Drooped-Nose and Plain Flaps. NACA RM L9G15, 1949.

9. Lindsey, W. F., Daley, Bernard N., and Humphreys, Milton D.: The Flow and Force Characteristics of Supersonic Airfoils at High Subsonic Speeds. NACA TN 1211, 1947.

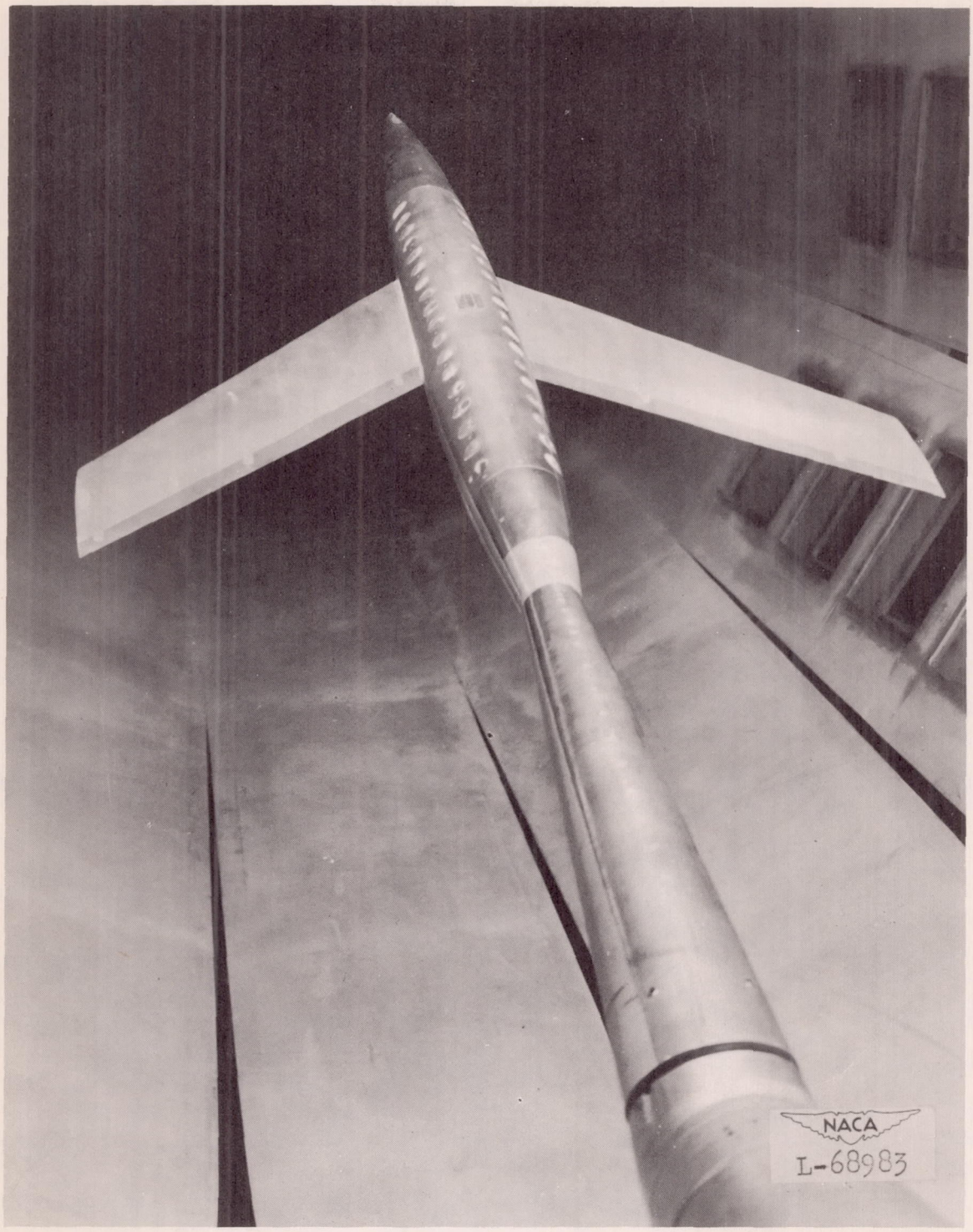

Figure 1.- Wing-fuselage combination mounted on the sting-support system in the 8-foot slotted test section.

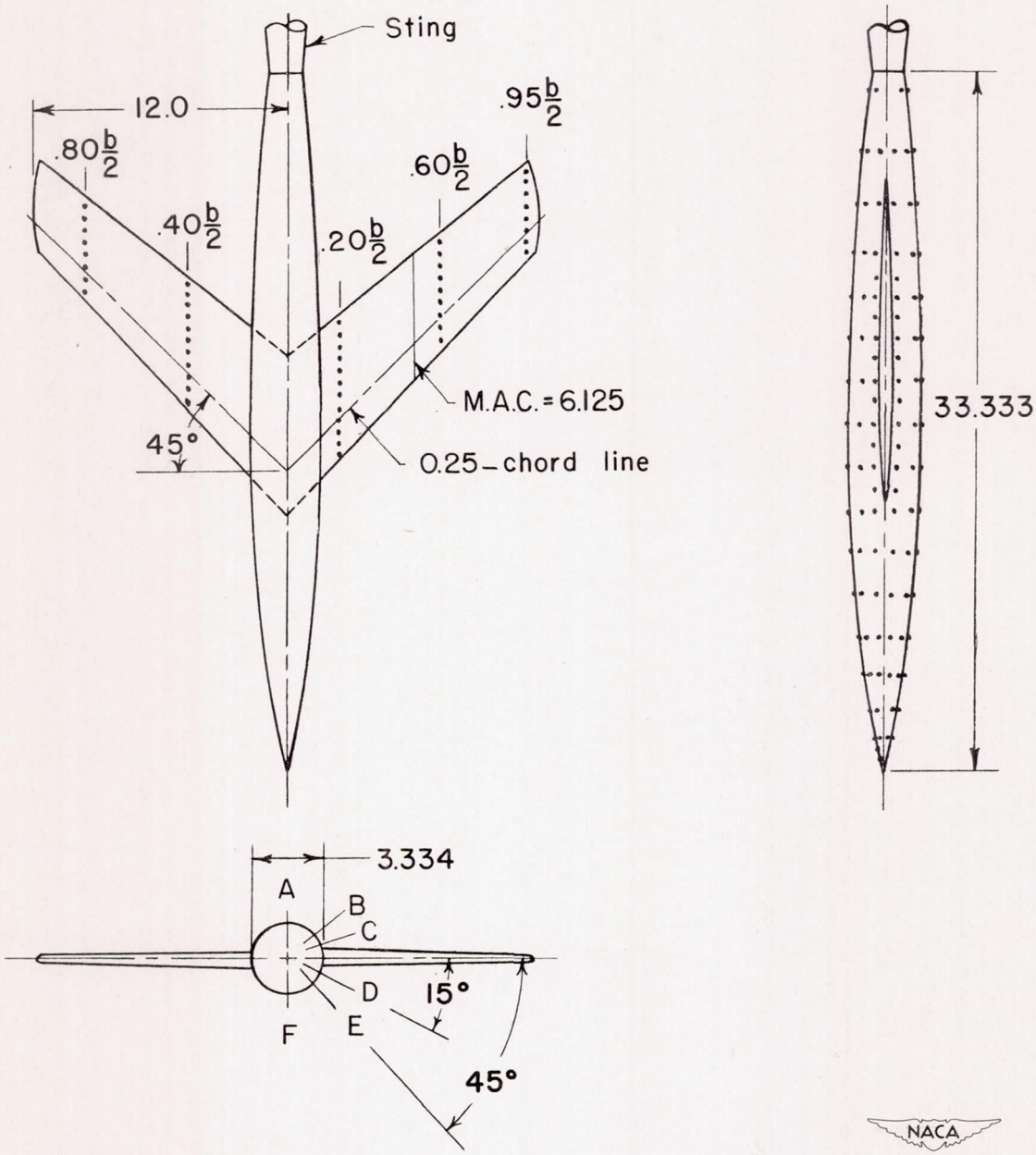

Figure 2.- Pressure model dimensions and orifice locations. All dimensions are in inches.

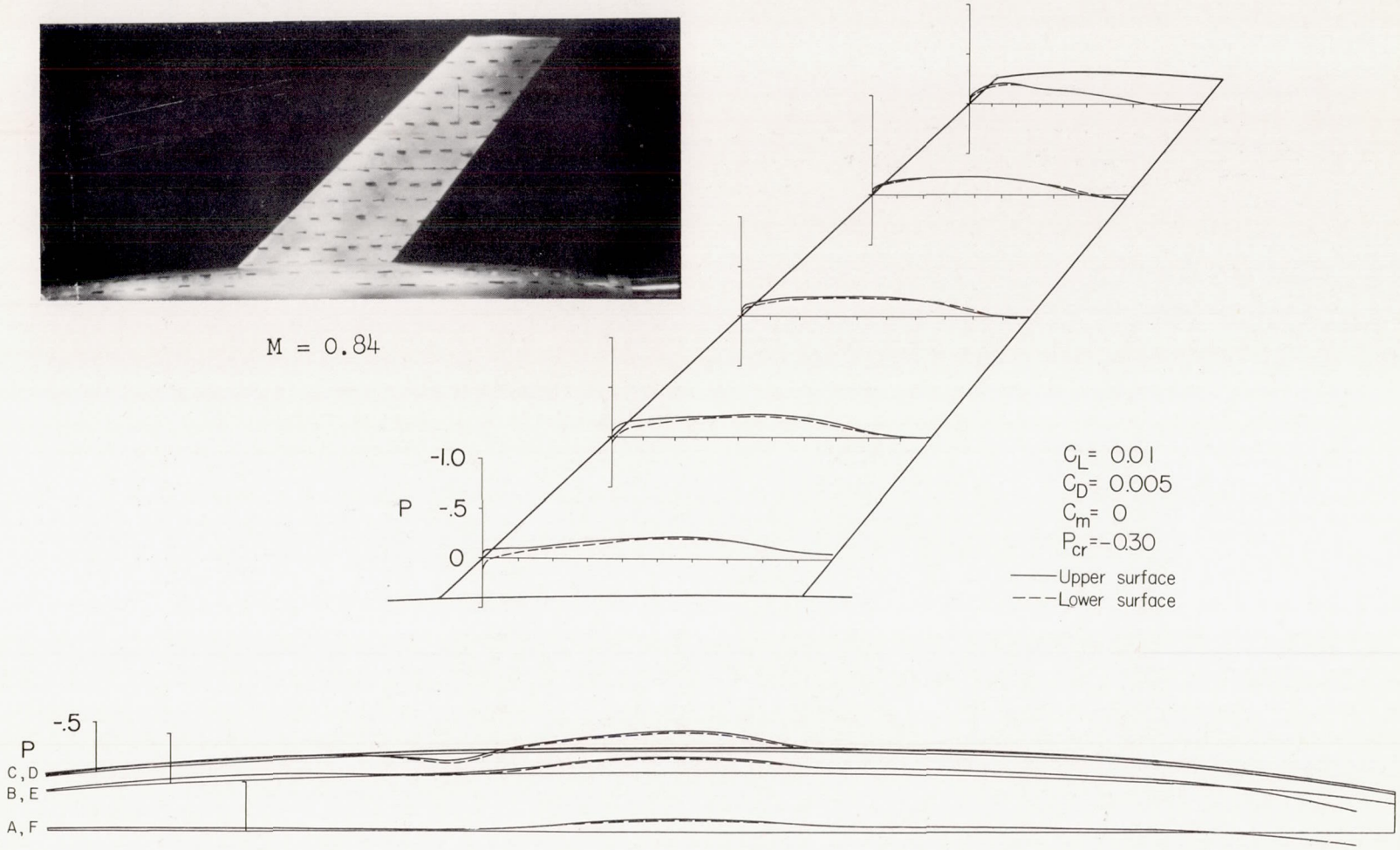

(a) M = 0.85.

Figure 3.- Pressure distributions, tuft patterns, and schlieren surveys. $\alpha = 0^{\circ}$.

L-74382

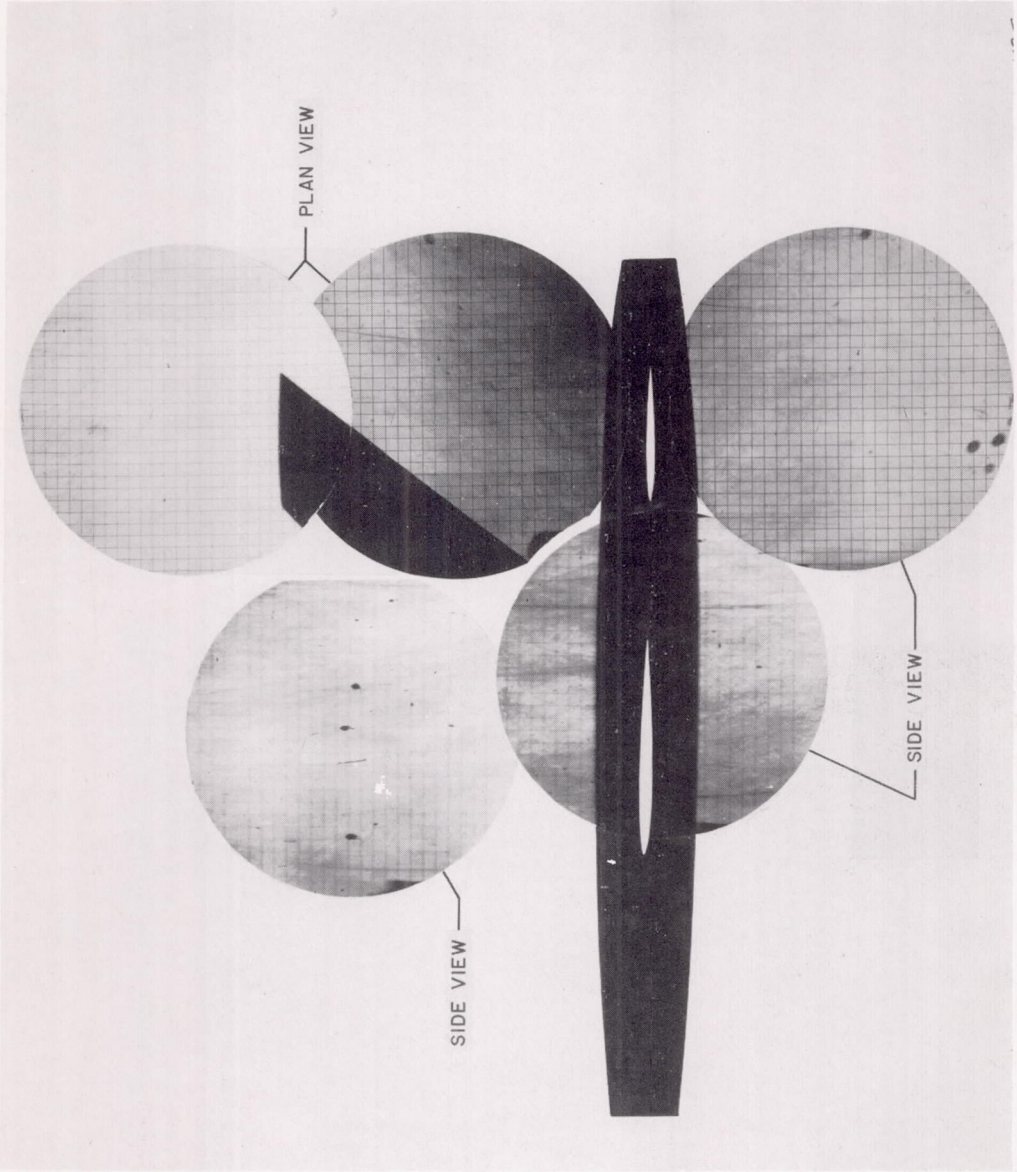

L-74383

(a) M = 0.84. Concluded.

Figure 3.- Continued.

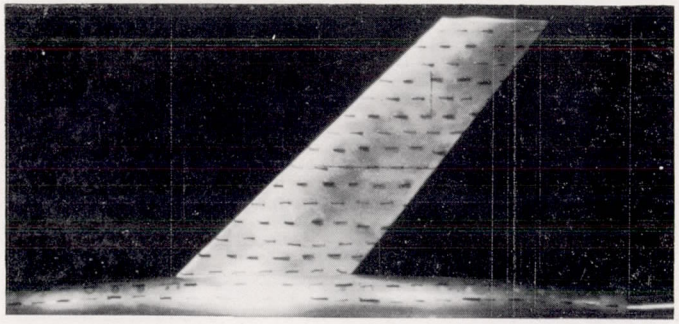

M = 0.89

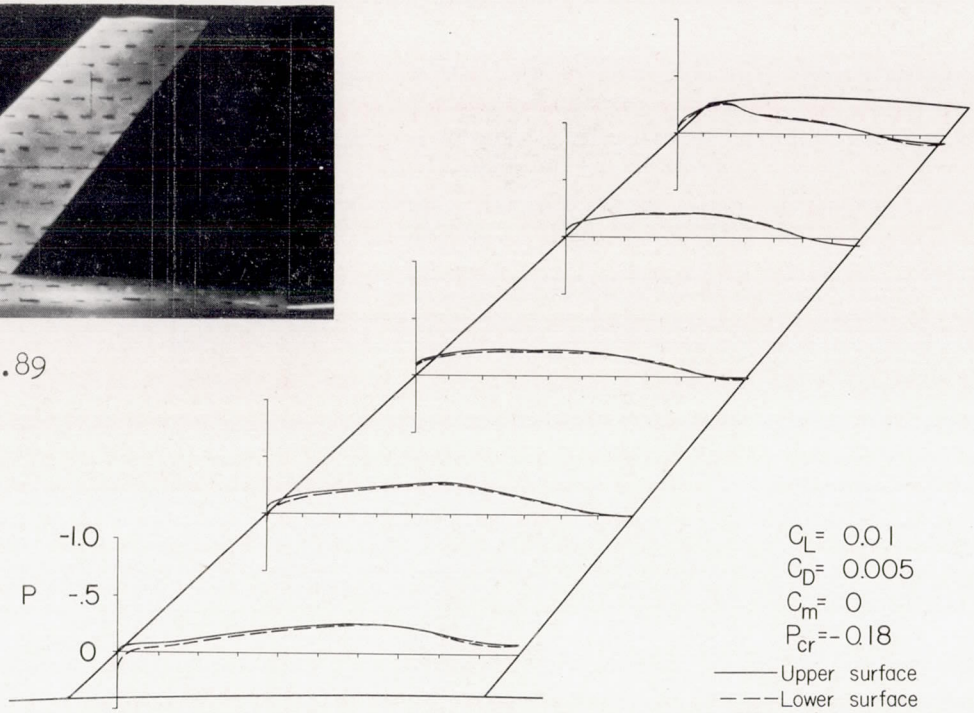

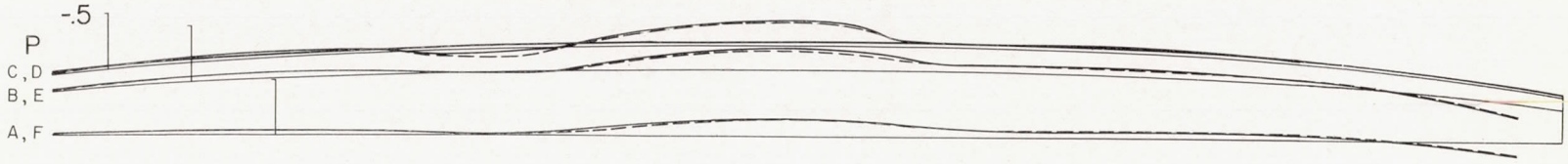

(b) M = 0.90.

Figure 3.- Continued.

NACA

L-74384

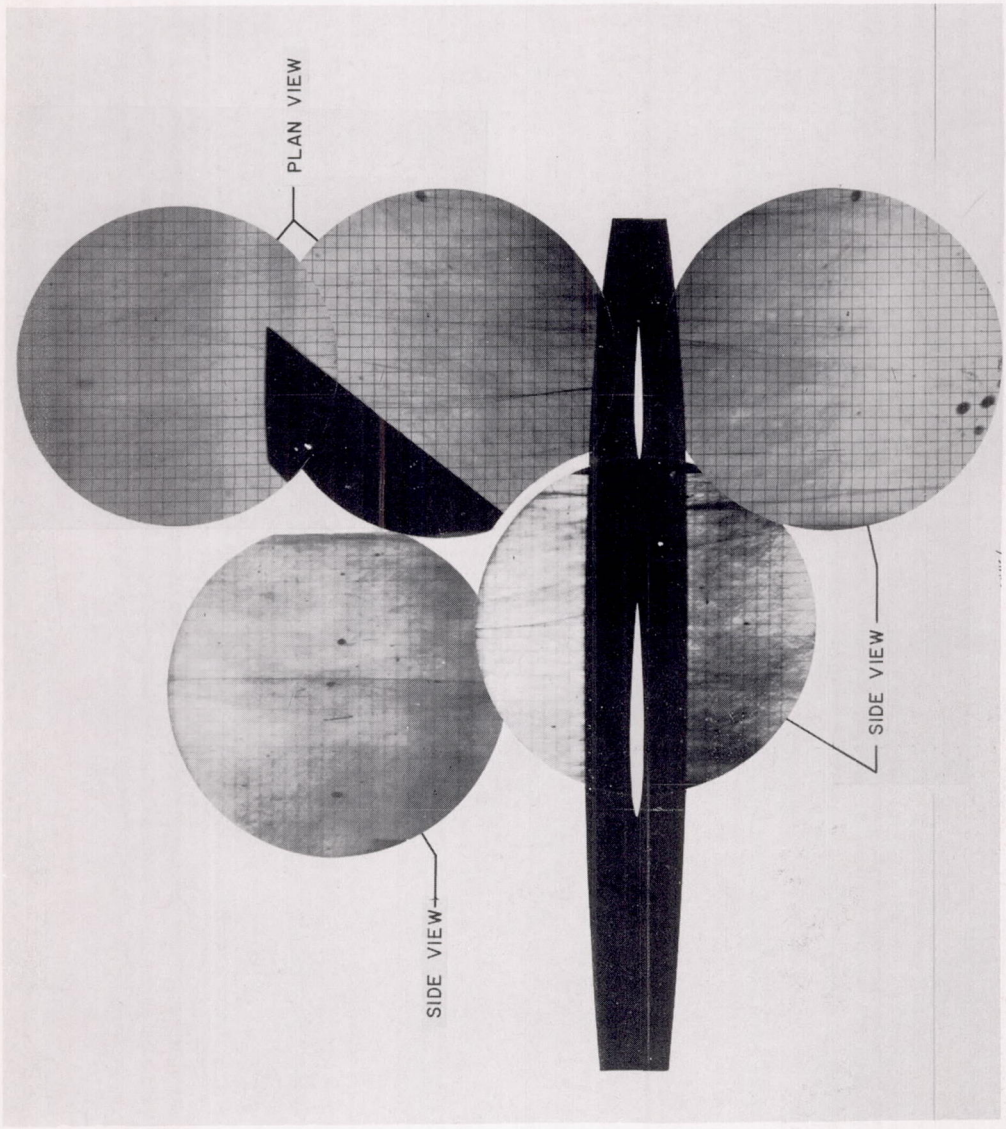

L-74385

(b) M = 0.89. Concluded.

Figure 3.- Continued.

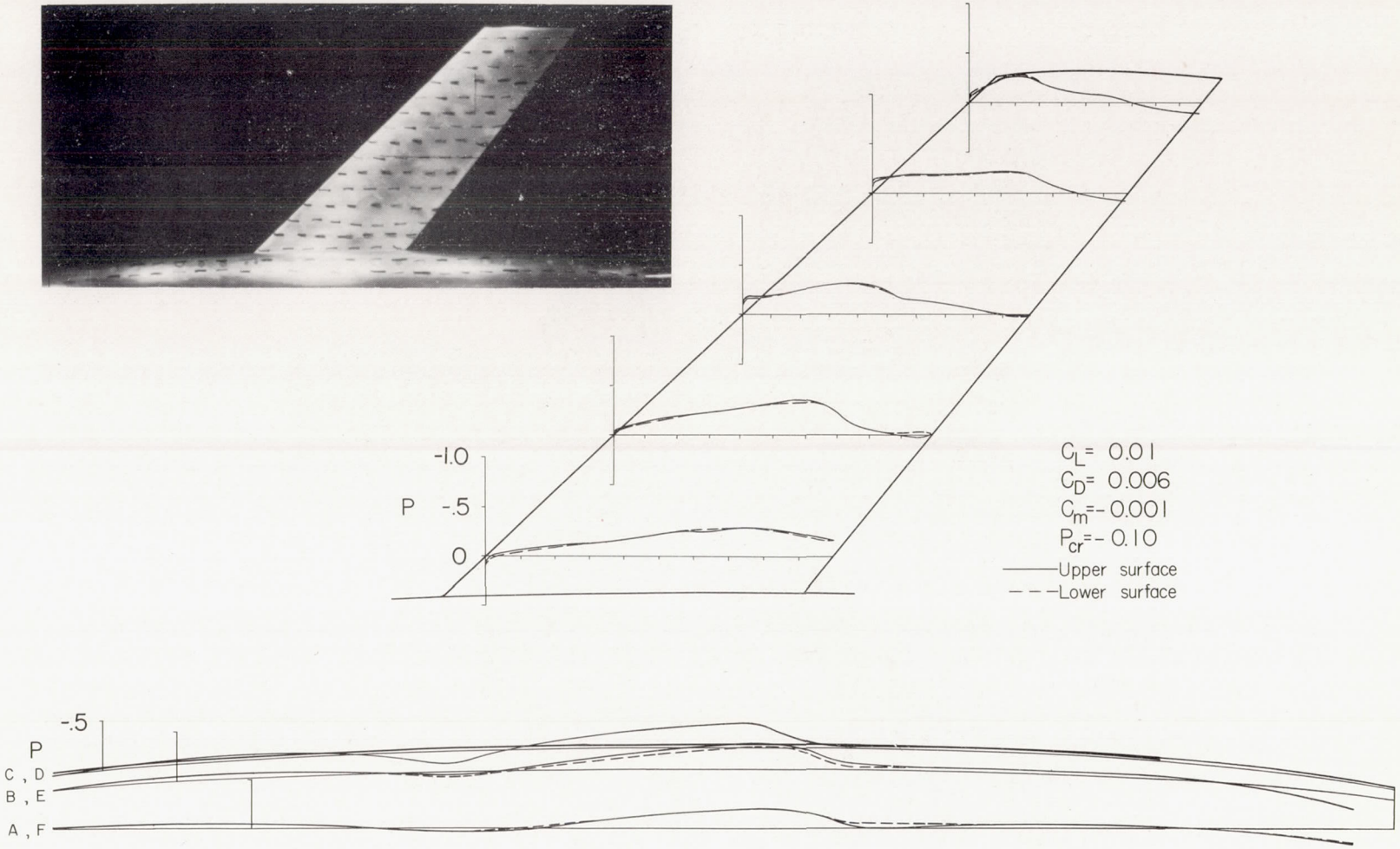

(c) M = 0.94.

Figure 3.- Continued.

L-74386

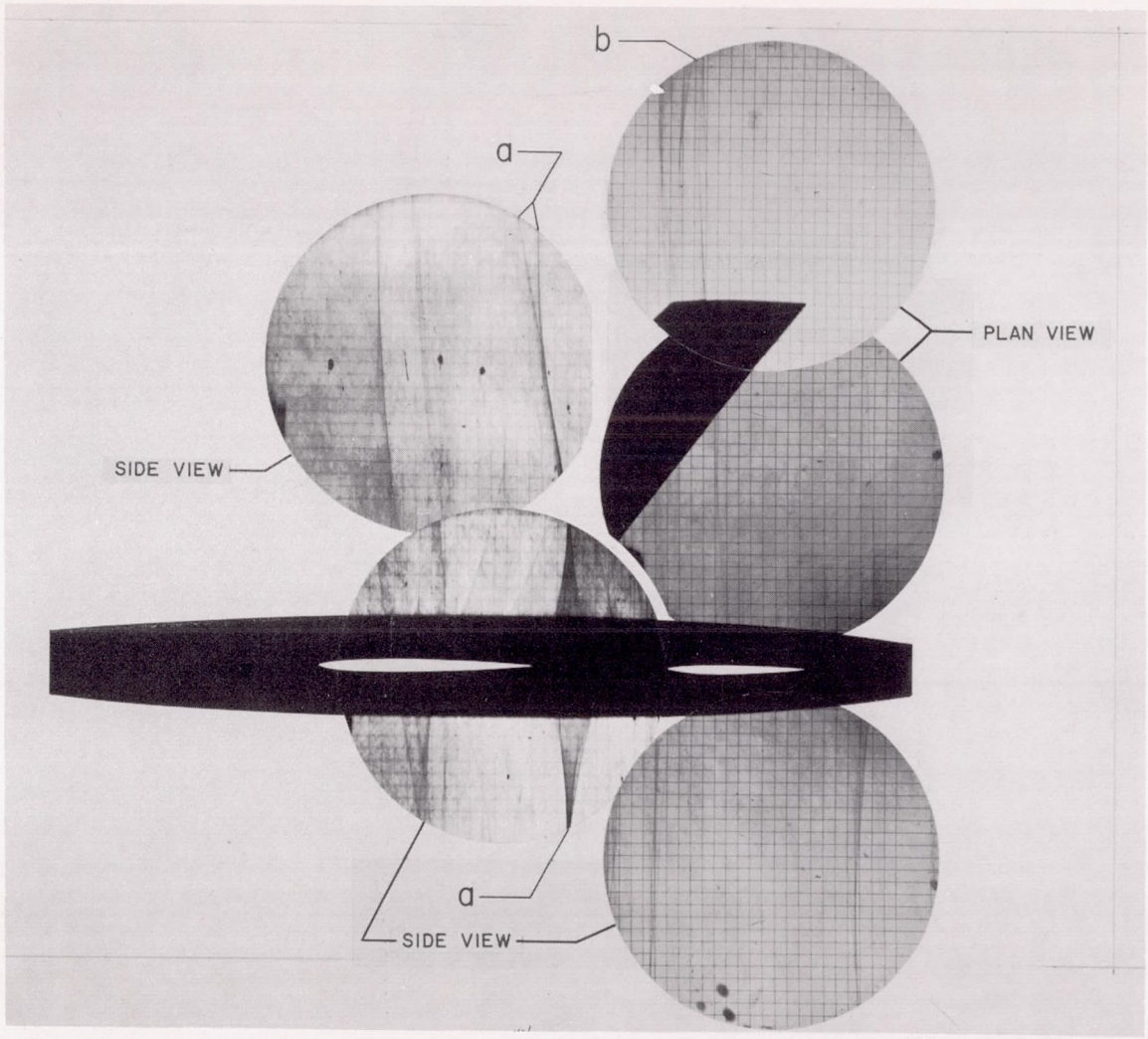

(c) M = 0.94. Concluded.

Figure 3.- Continued.

NACA

L-74387

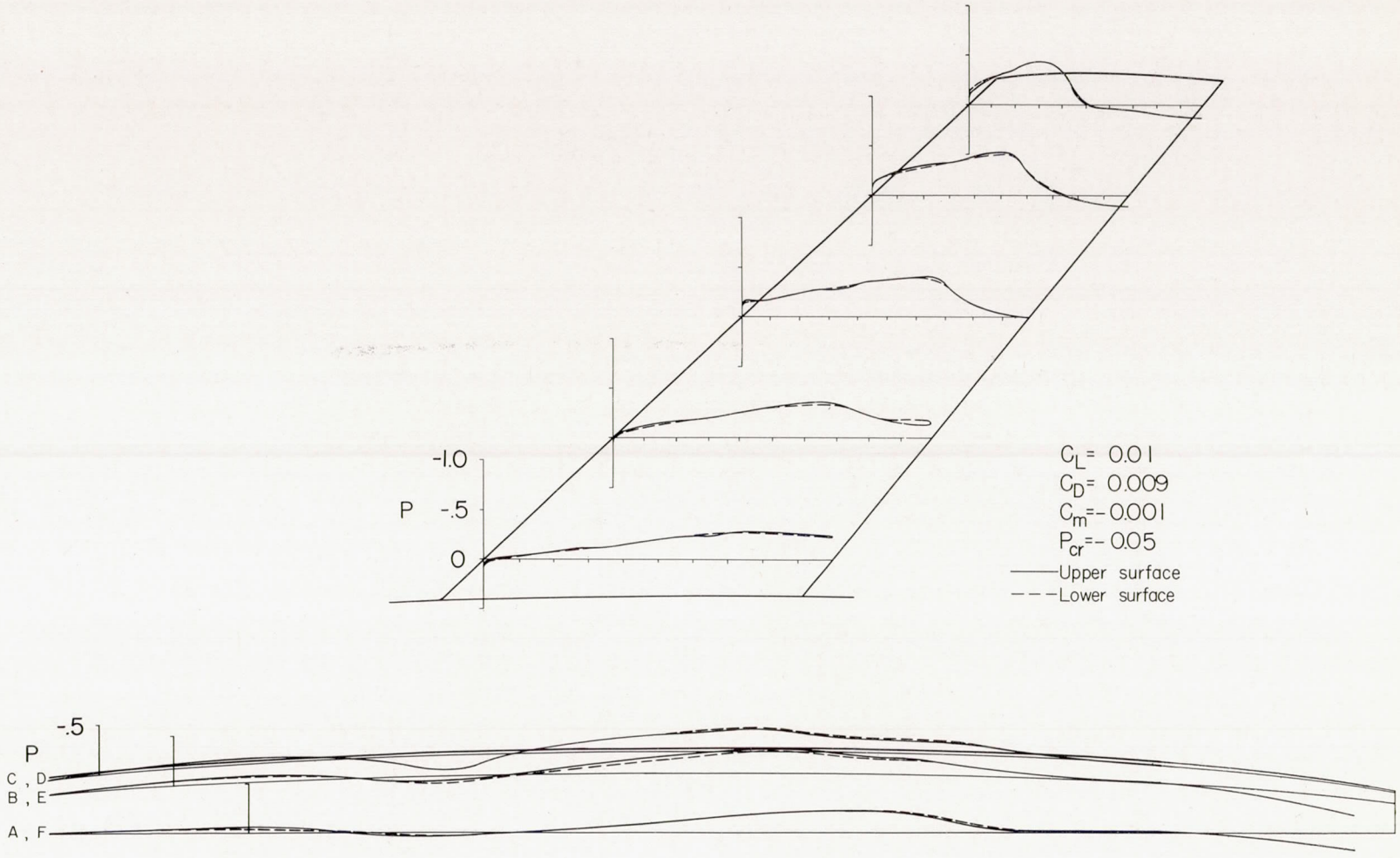

(d) M = 0.97.

Figure 3.- Continued.

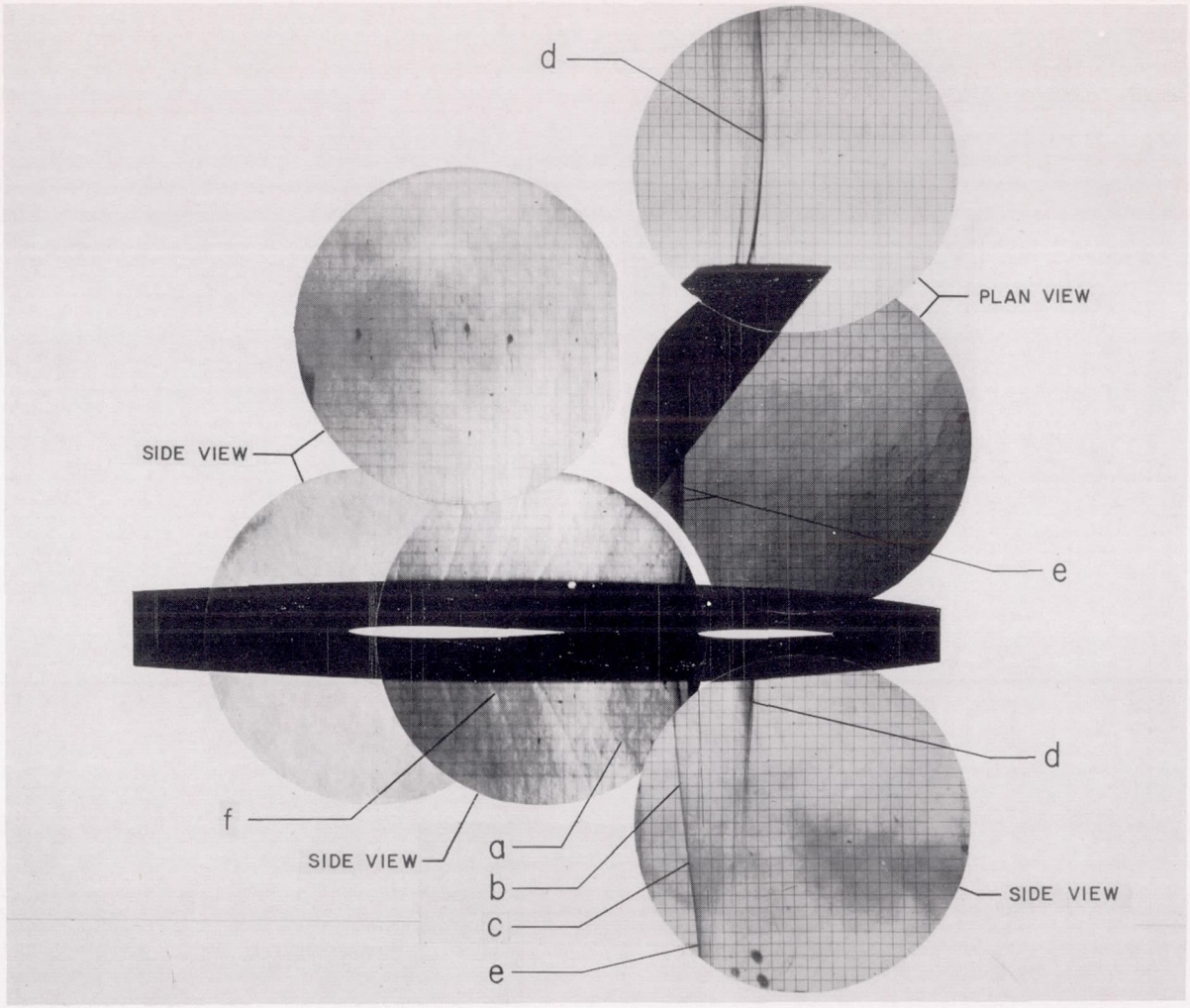

(d) M = 0.97. Concluded.

Figure 3.- Continued.

NACA

L-74388

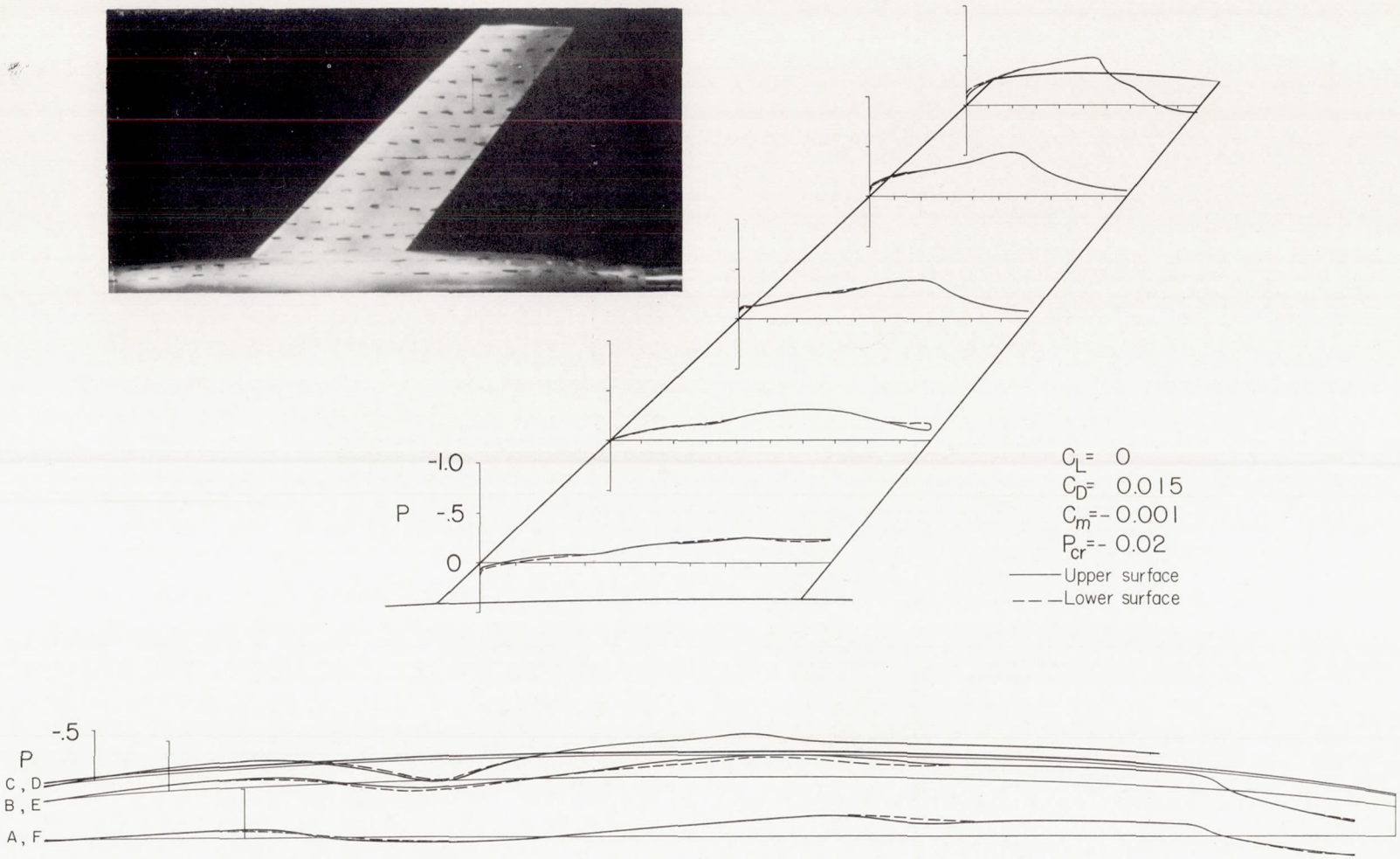

(e) M = 0.99.

Figure 3.- Continued.

NACA

L-74389

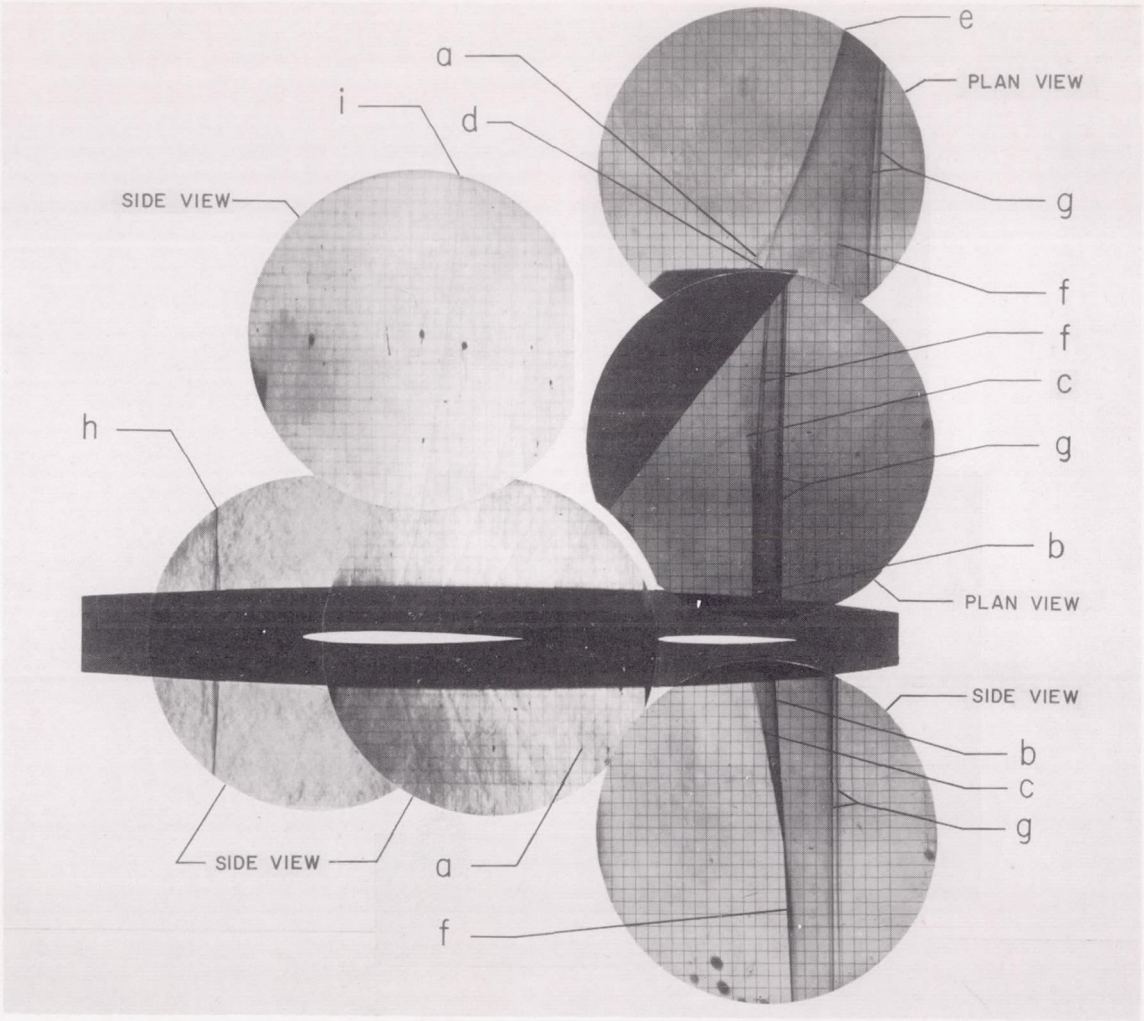

(e) M = 0.99. Concluded.

Figure 3.- Continued.

L-74390

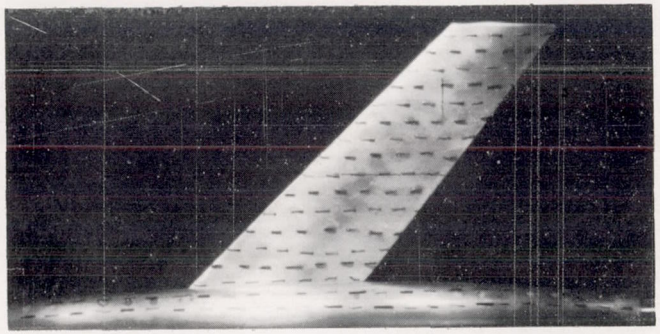

M = 1.01

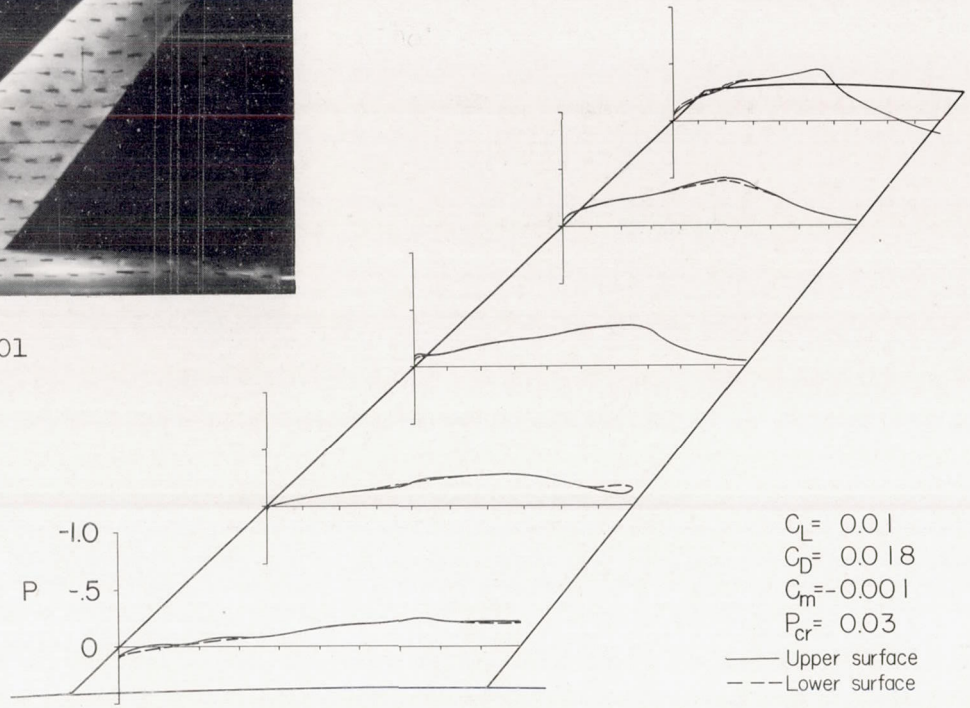

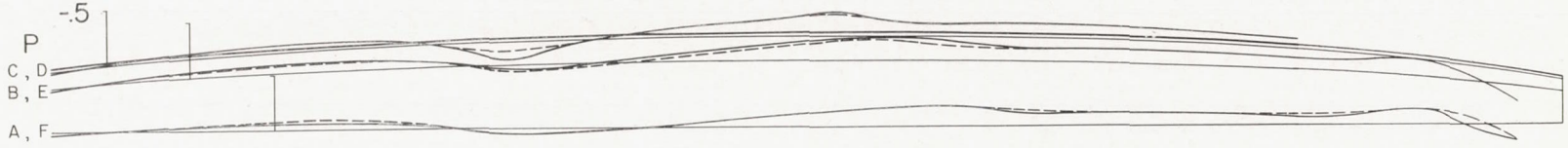

(f) M = 1.02.

Figure 3.- Continued.

NACA

L-74391

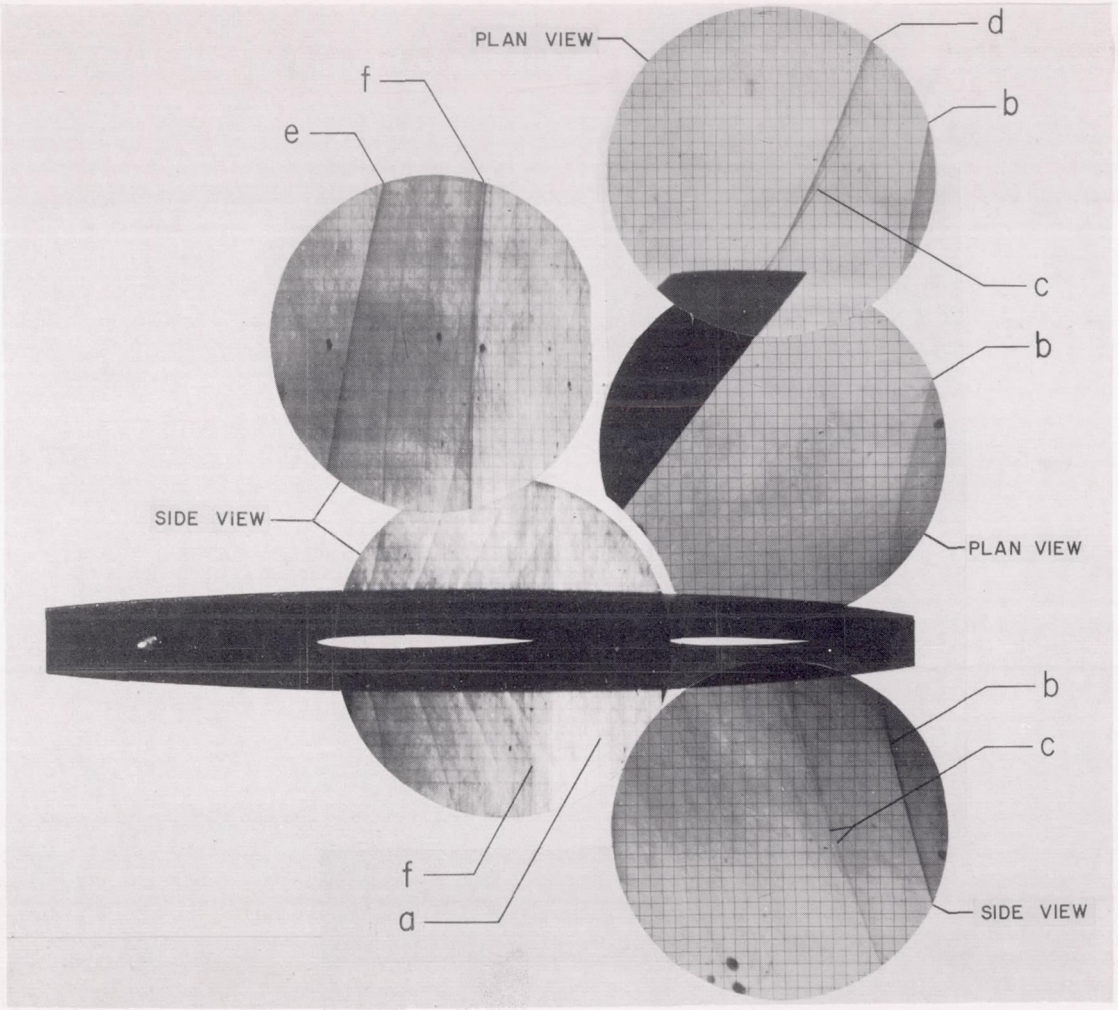

(f) M = 1.02. Concluded.

Figure 3.- Continued.

NACA
L-74392

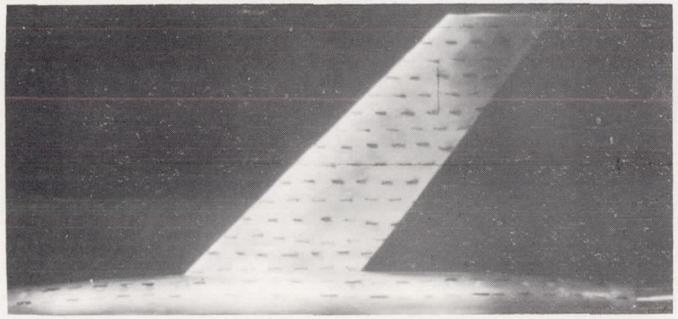

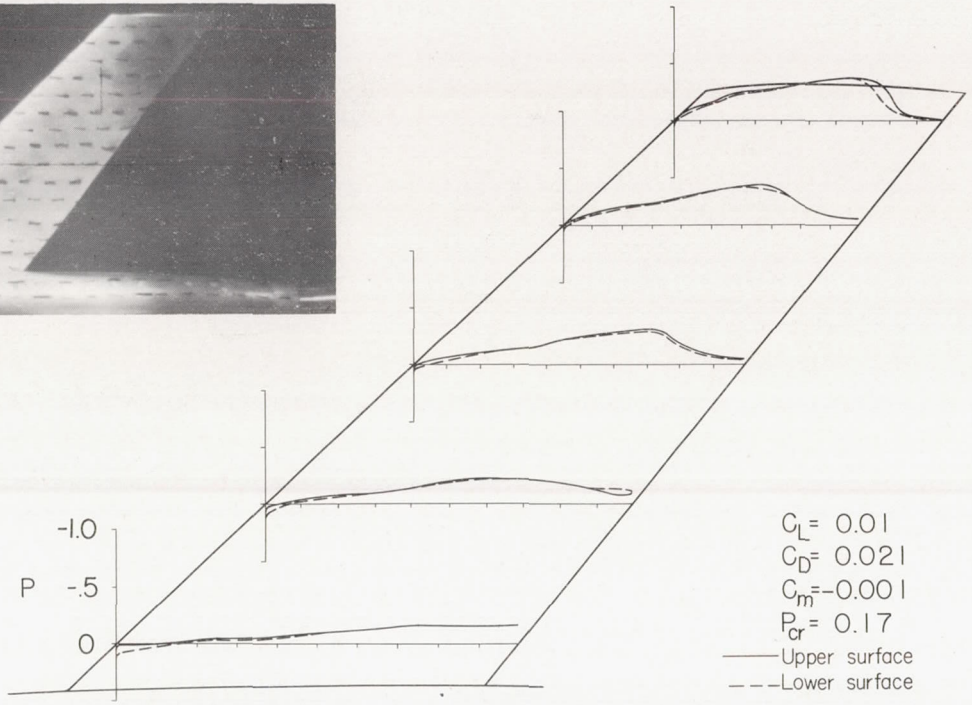

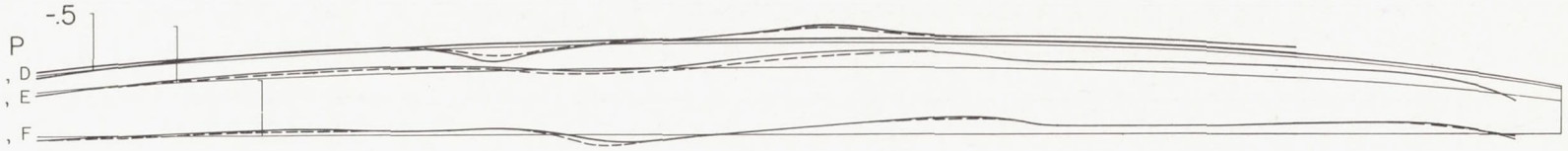

(g) M = 1.11.

Figure 3.- Continued.

NACA

L-74393

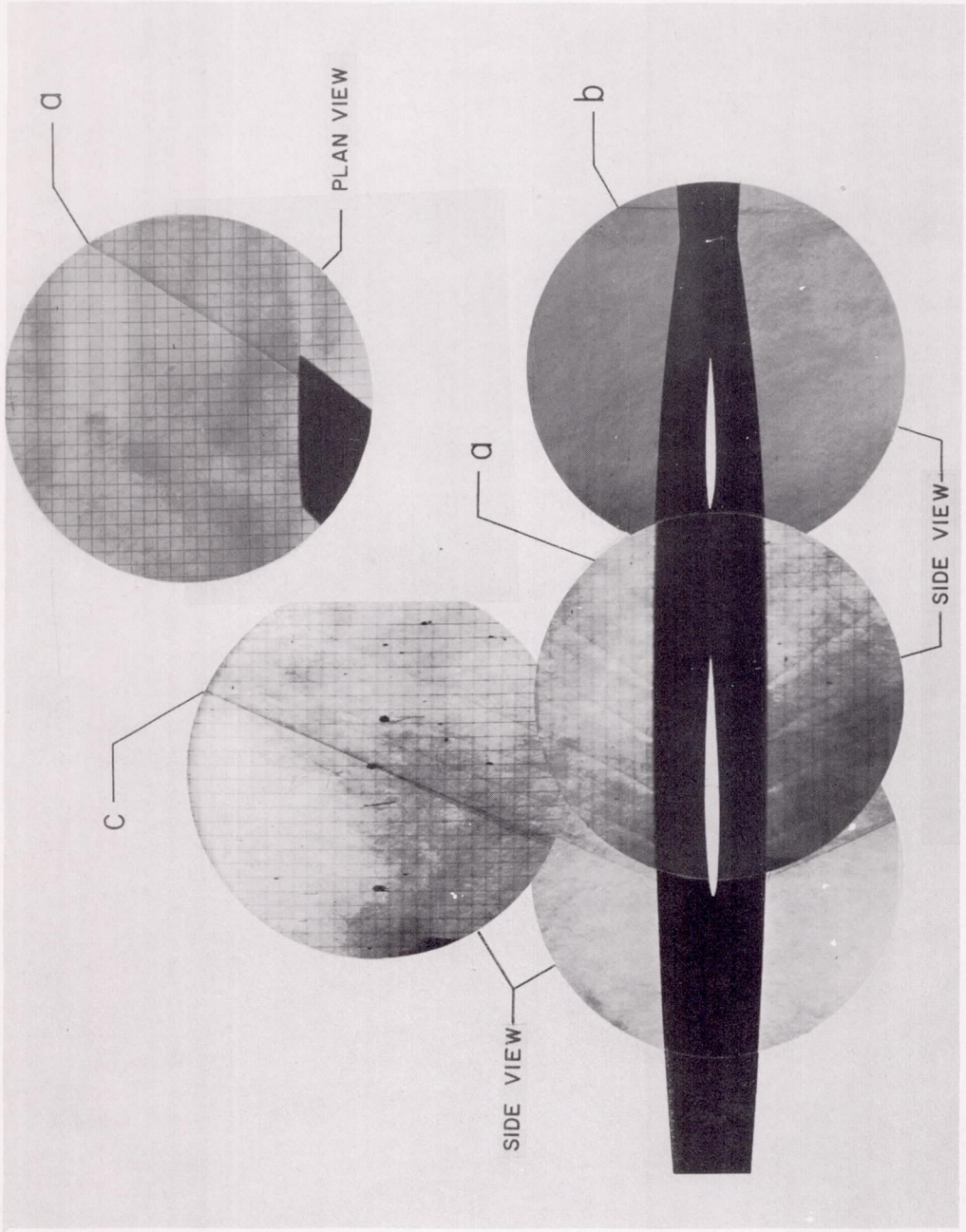

(g) M = 1.11. Concluded.

Figure 3.- Concluded.

L-74394

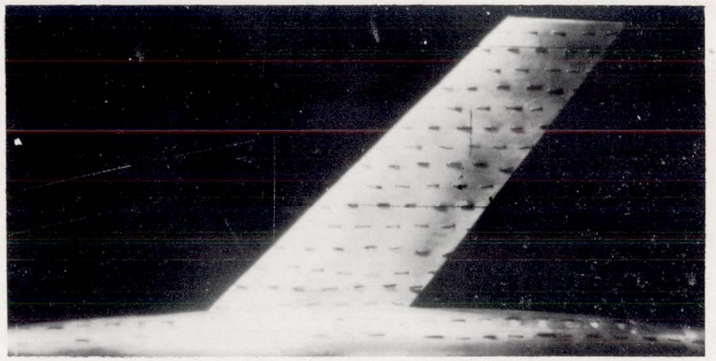

M = 0.84

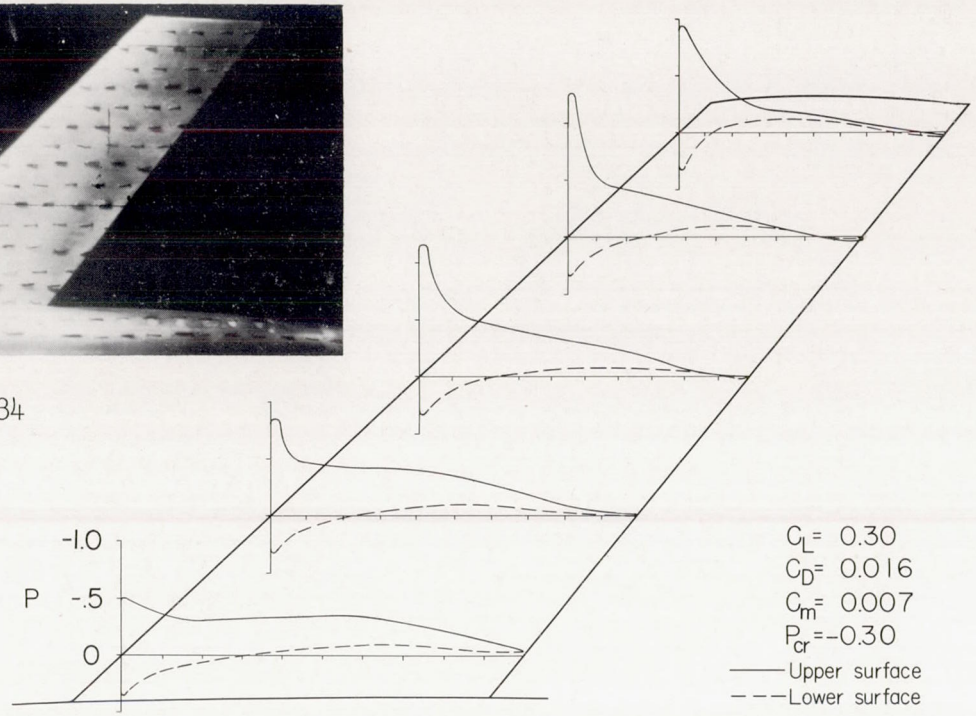

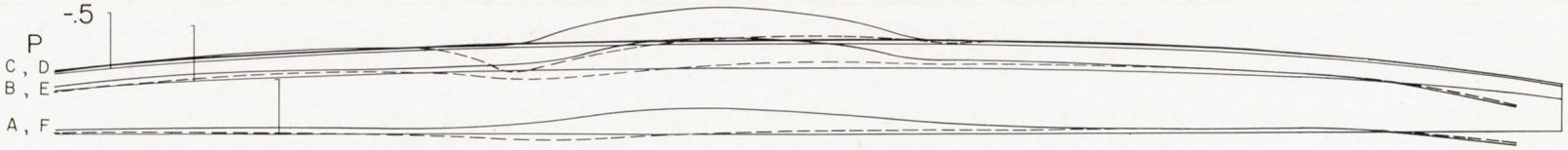

(a) M = 0.85.

Figure 4.- Pressure distributions, tuft patterns, and schlieren surveys. $\alpha = 4^{\circ}$.

L-74395

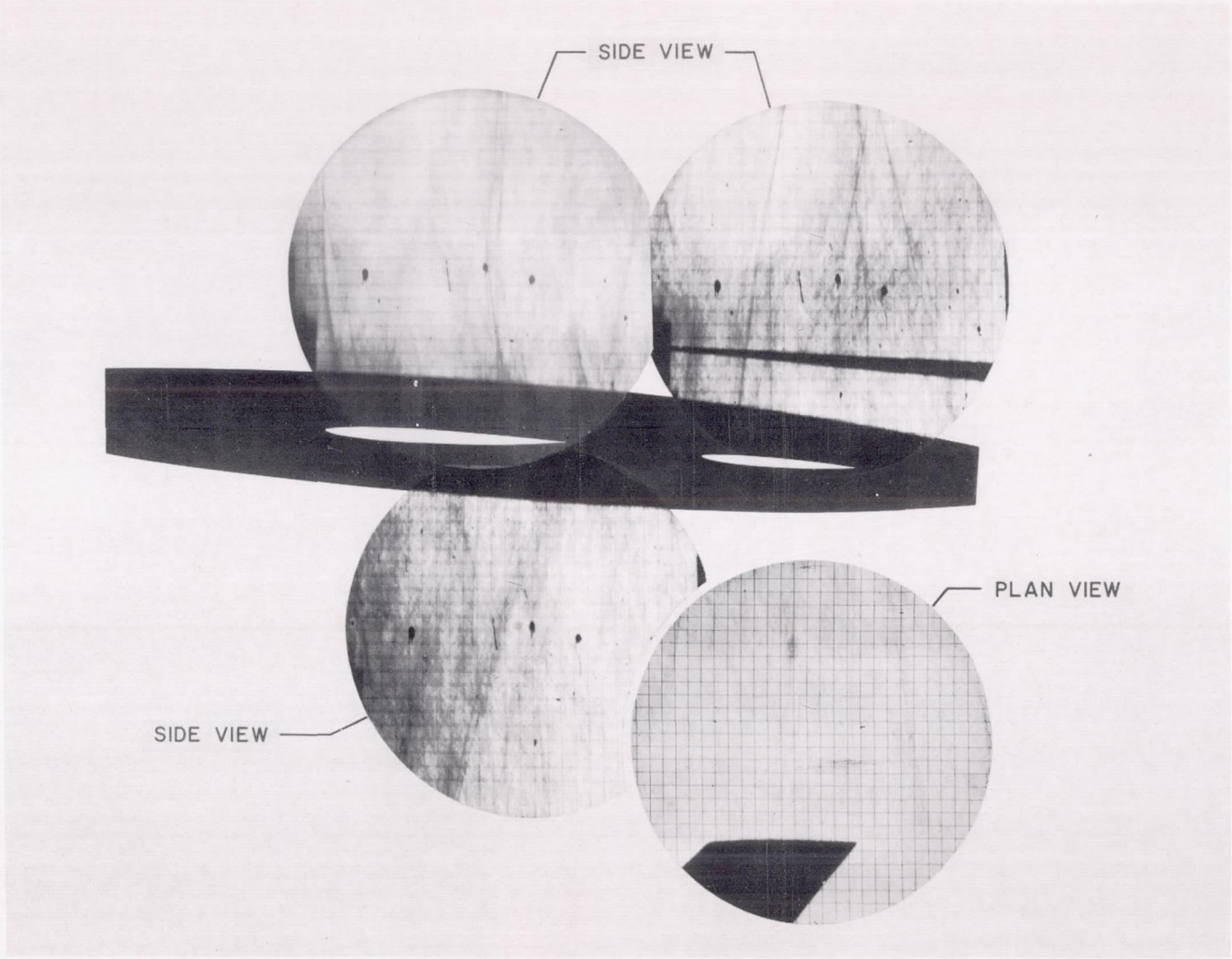

(a) M = 0.84. Concluded.

Figure 4.- Continued.

NACA

L-74396

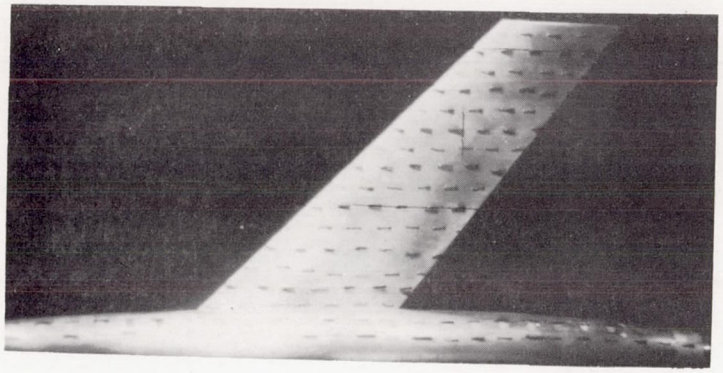

M = 0.89

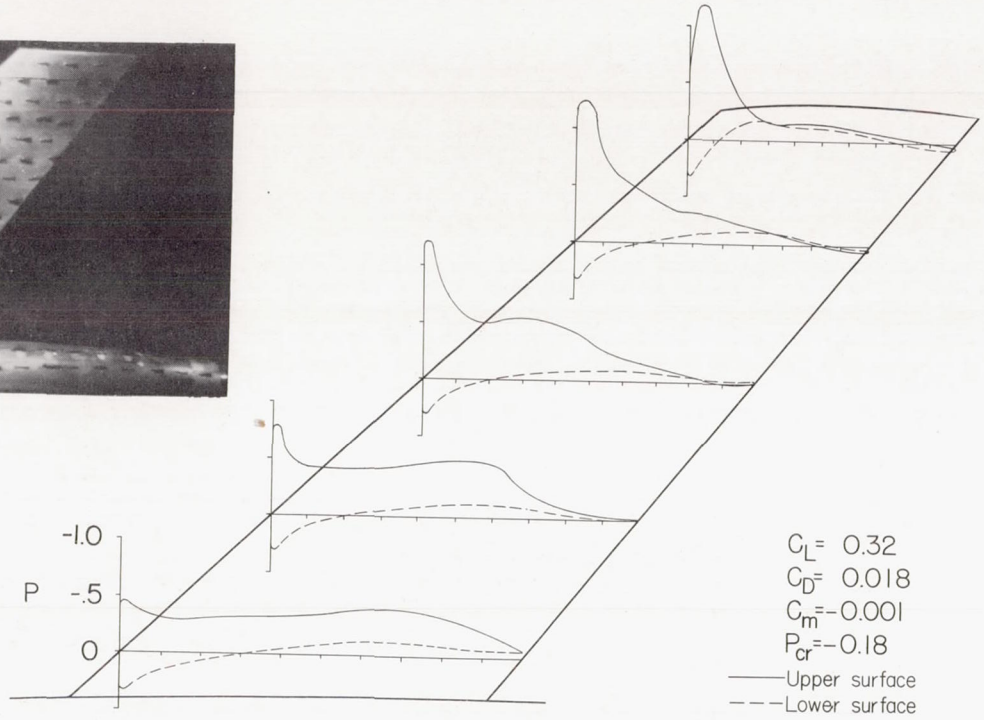

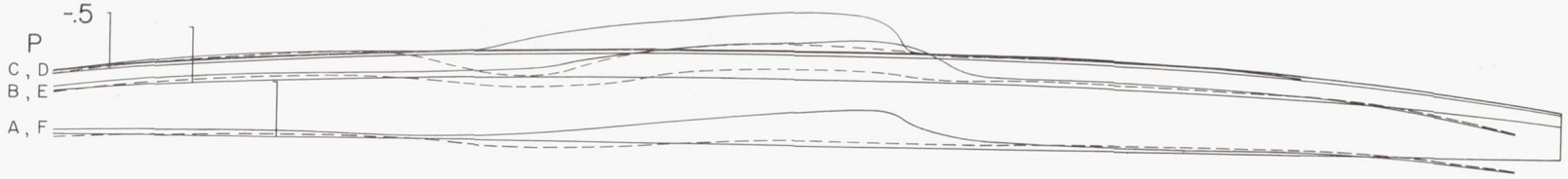

(b) M = 0.90.

Figure 4.- Continued.

L-74397

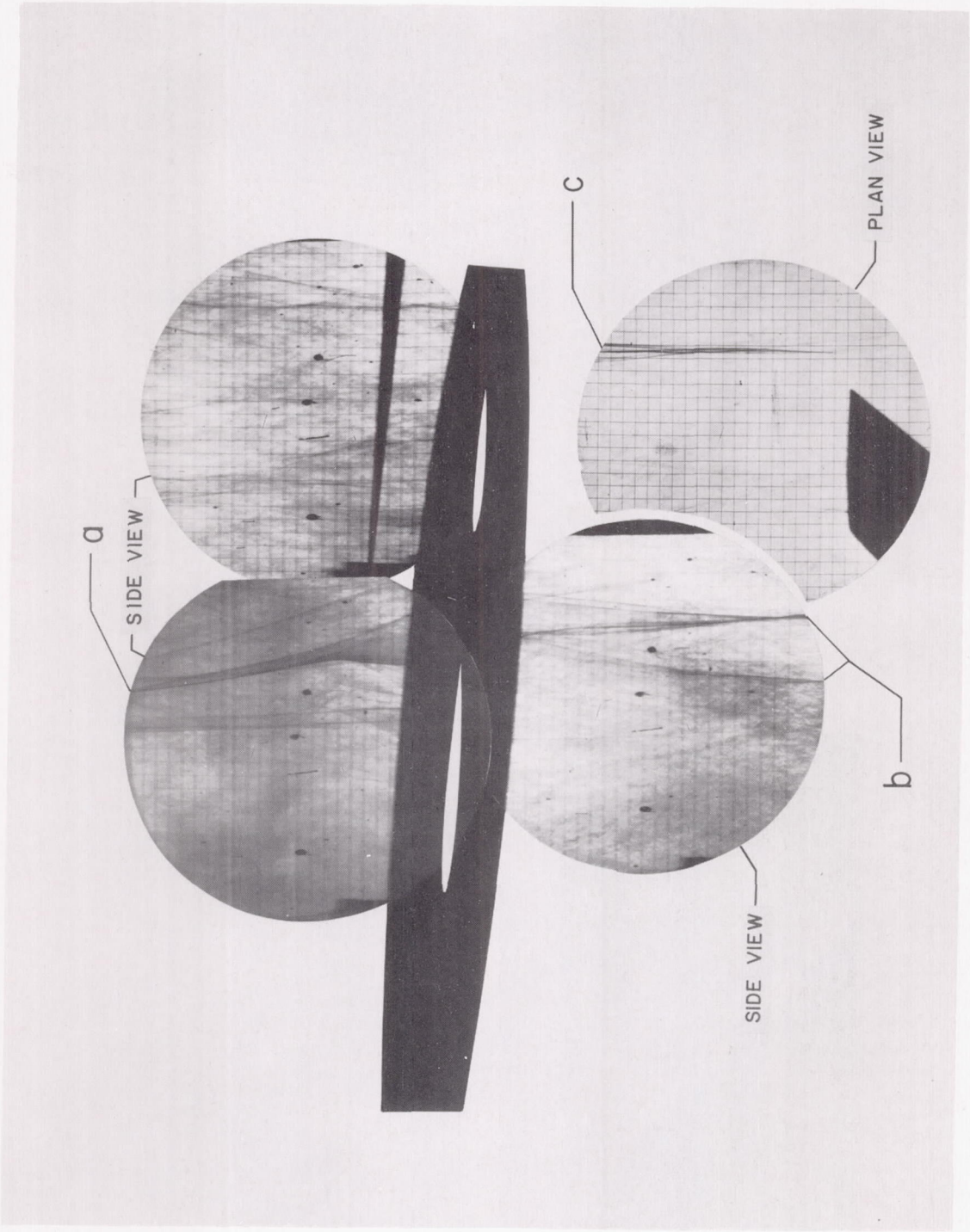

L-74398

(b) M = 0.89. Concluded.

Figure 4.- Continued.

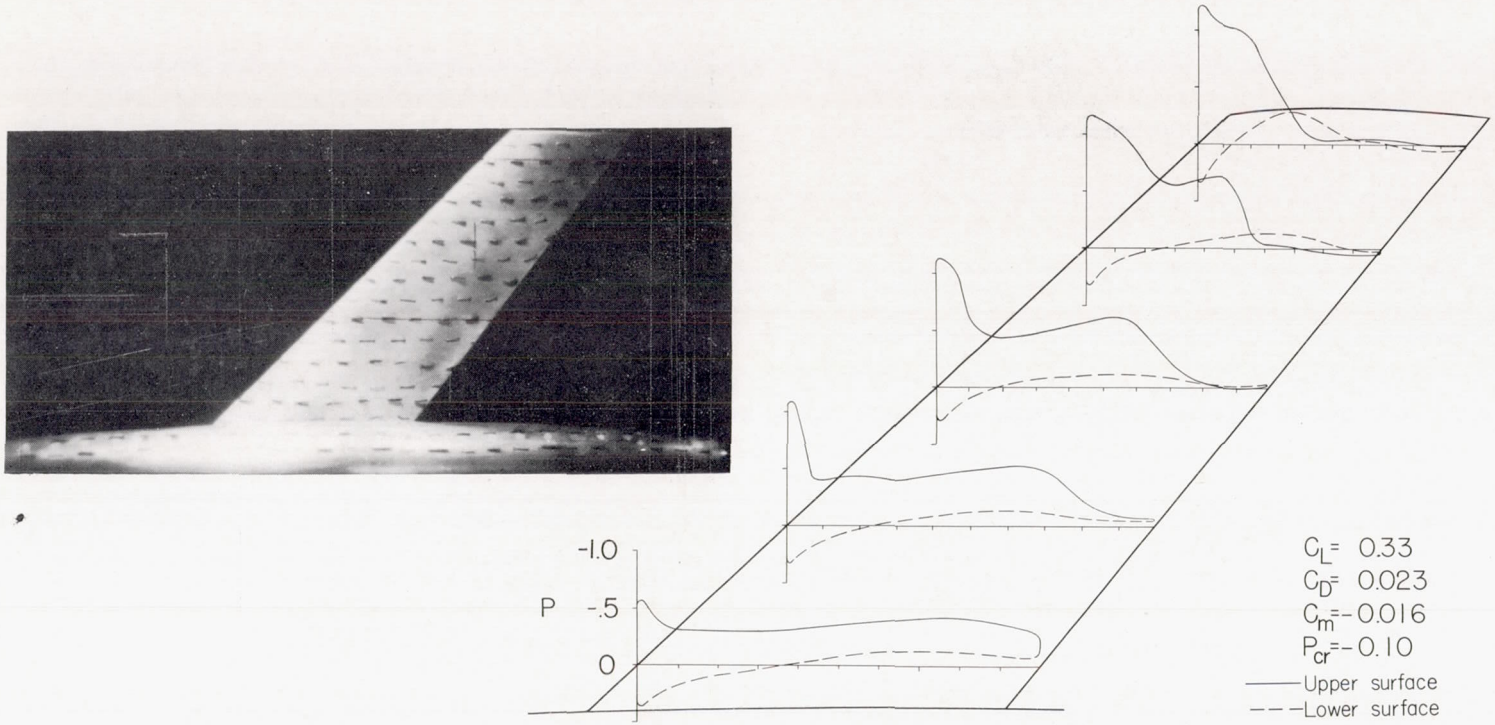

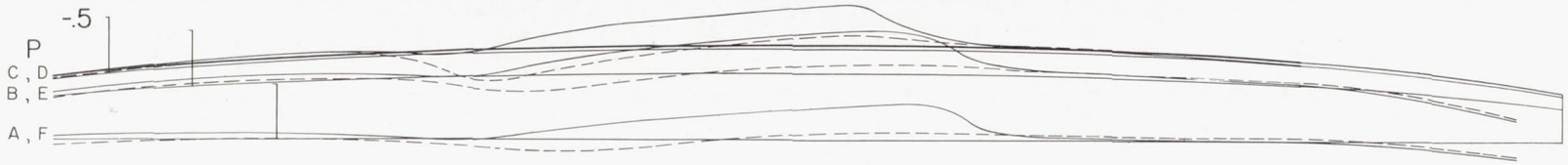

(c) M = 0.94.

Figure 4.- Continued.

L-74399

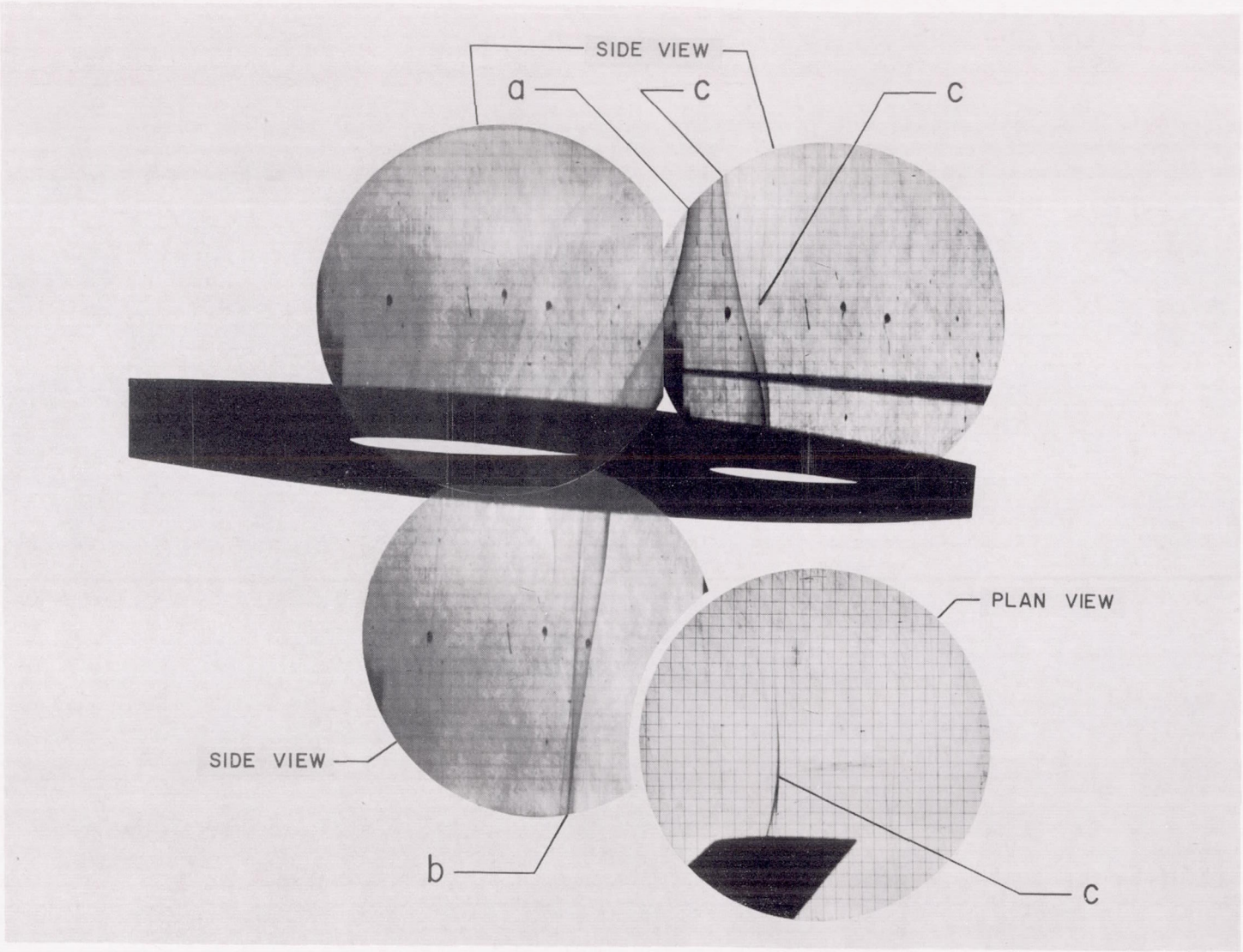

(c) M = 0.94. Concluded.

Figure 4.- Continued.

NACA

L-74400

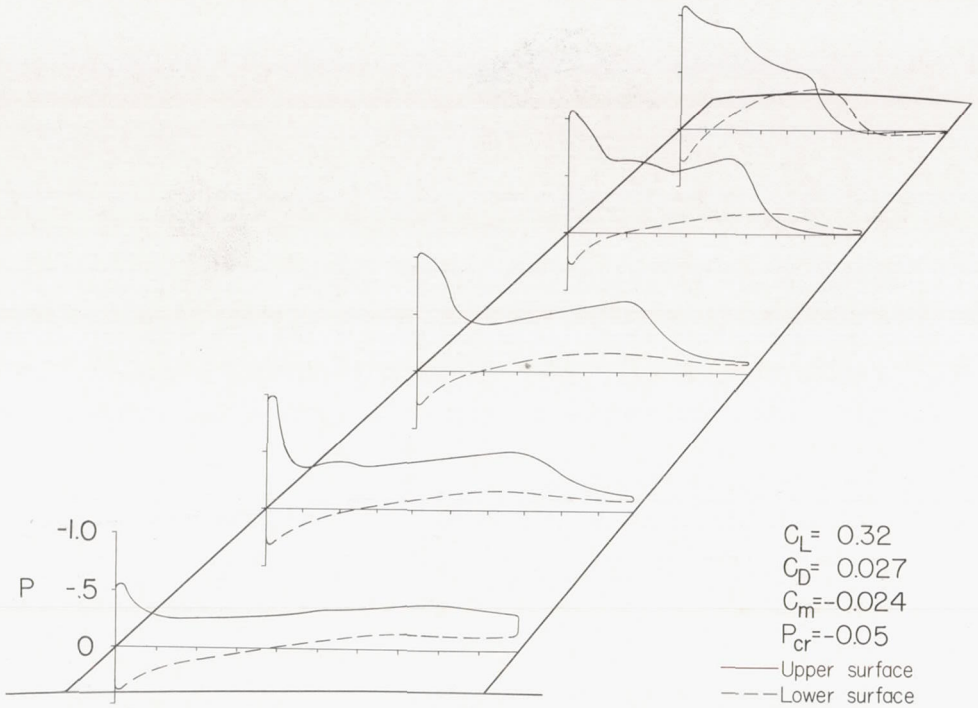

(d) M = 0.97.

Figure 4.- Continued.

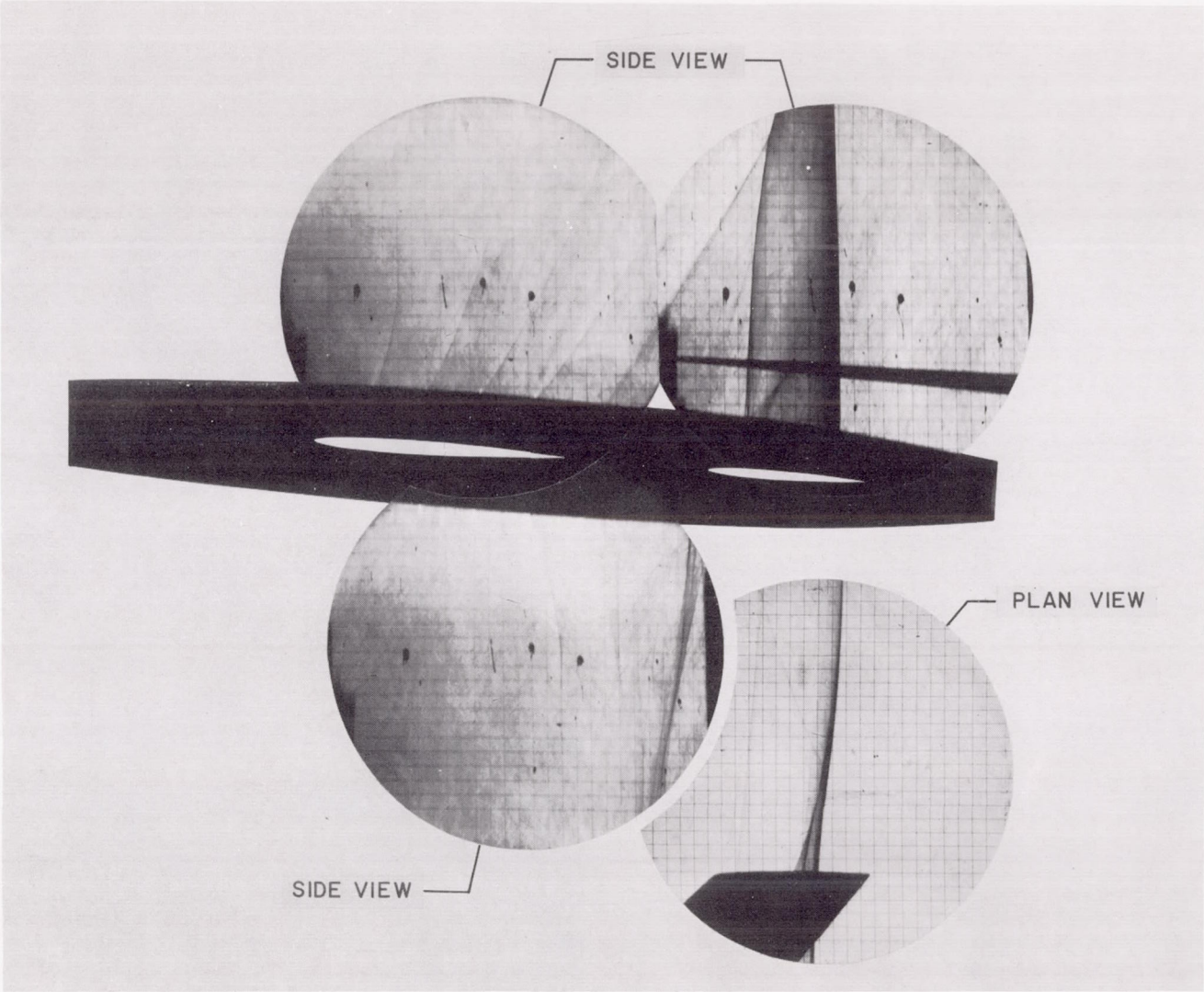

(d) M = 0.97. Concluded.

Figure 4.- Continued.

NACA

L-74401

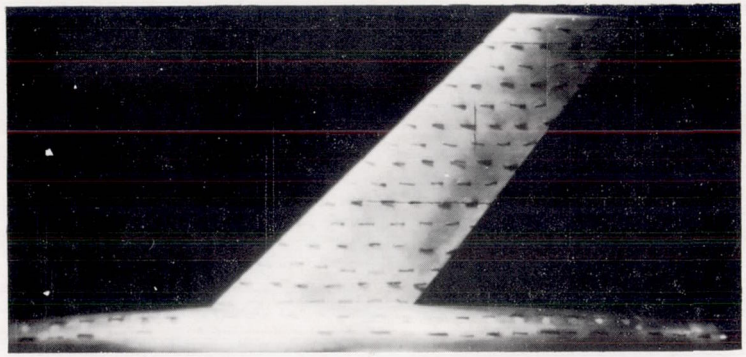

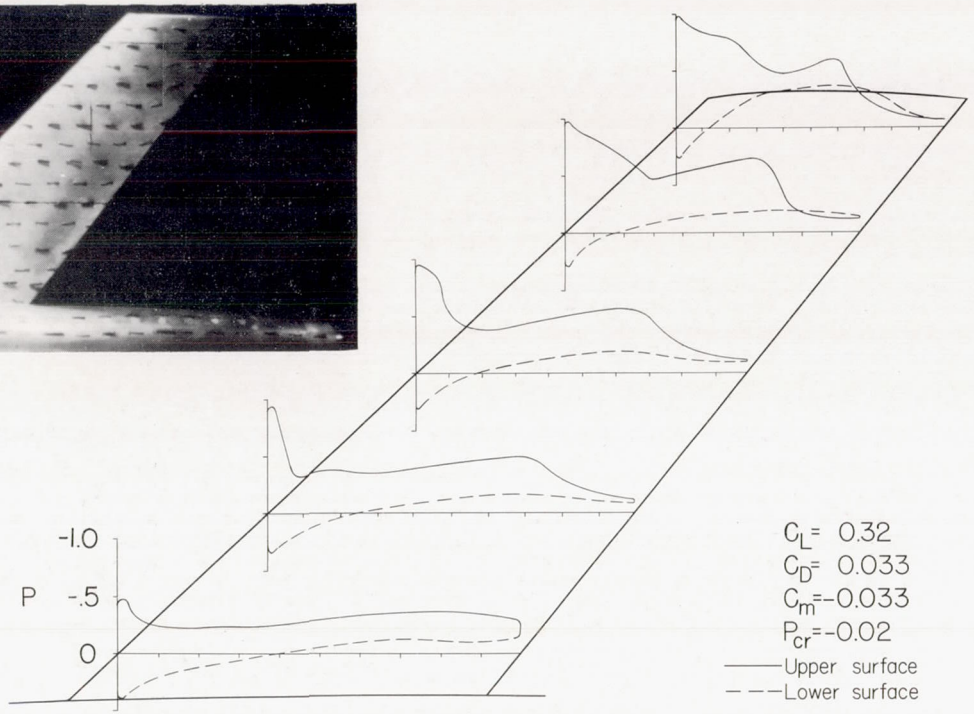

(e) M = 0.99.

Figure 4.- Continued.

NACA

L-74402

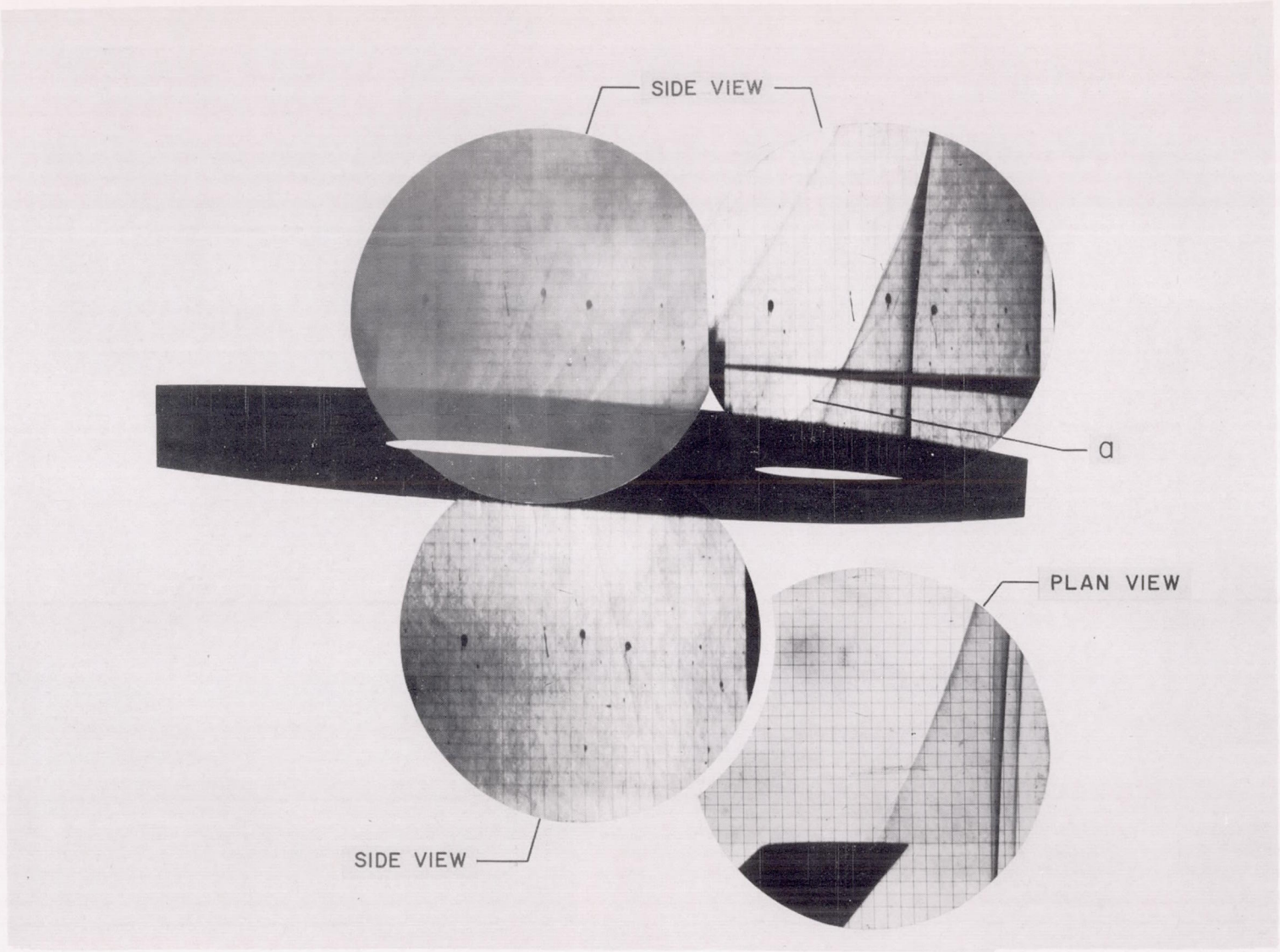

(e) M = 0.99. Concluded.

Figure 4.- Continued.

NACA

L-714103

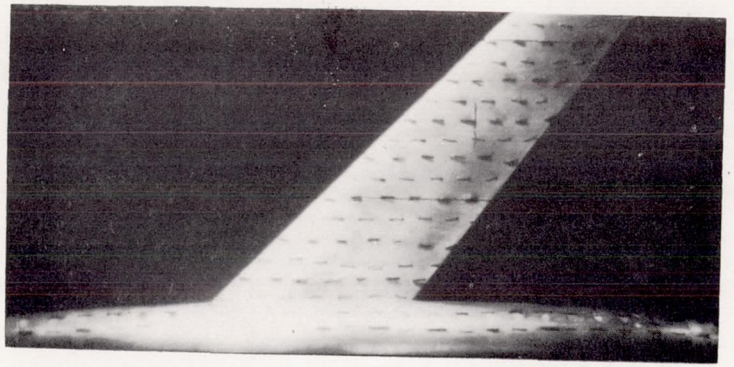

M = 1.01

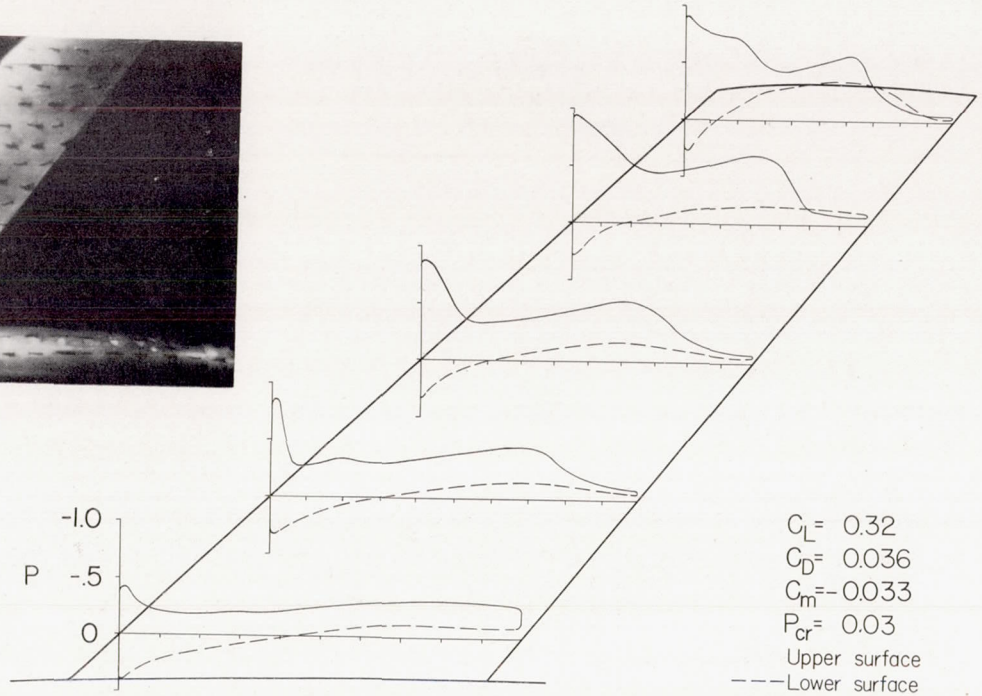

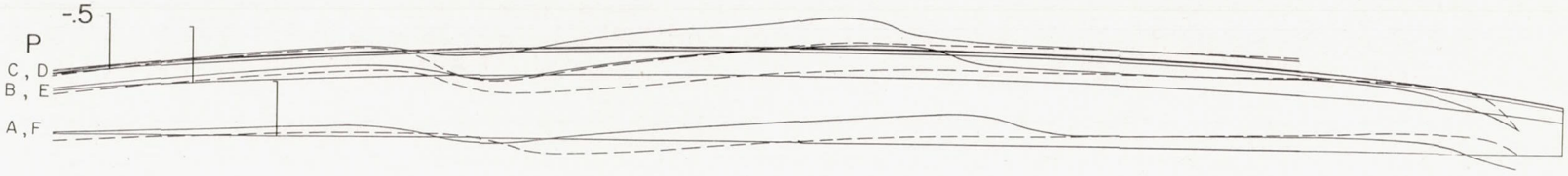

(f) M = 1.02.

Figure 4.- Continued.

L-74404

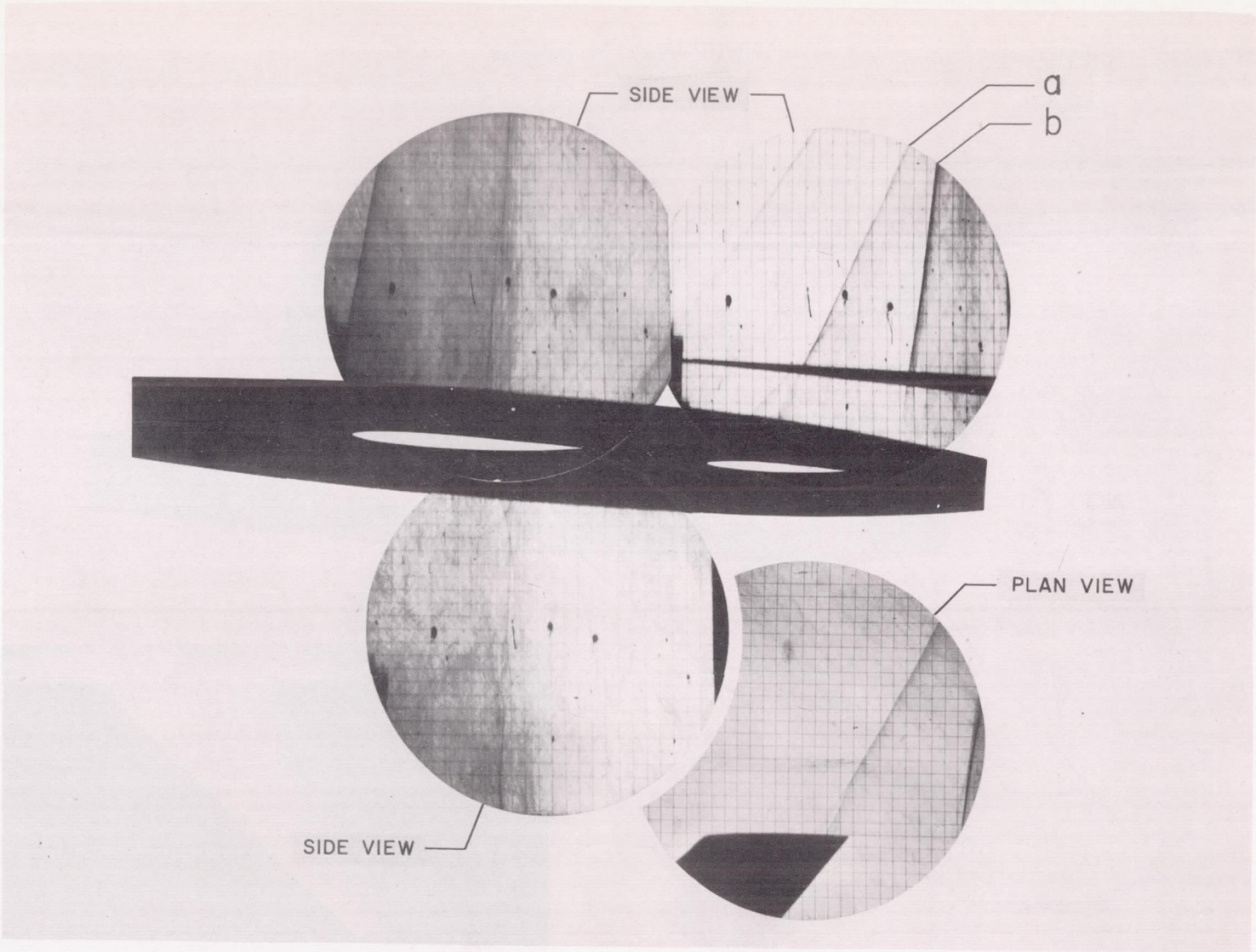

(f) M = 1.02. Concluded.

Figure 4.- Continued.

L-74405

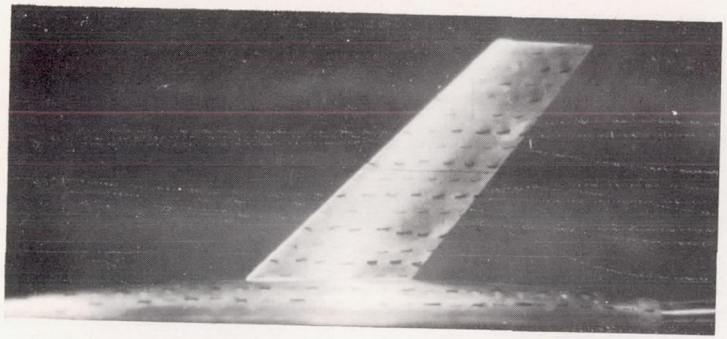

M = 0.79

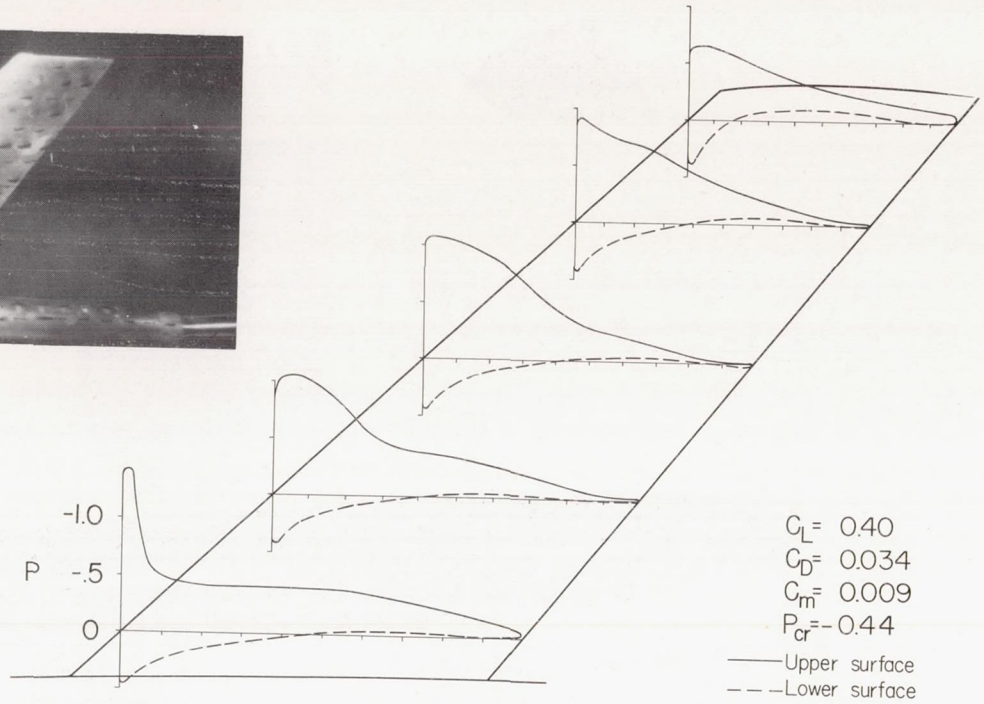

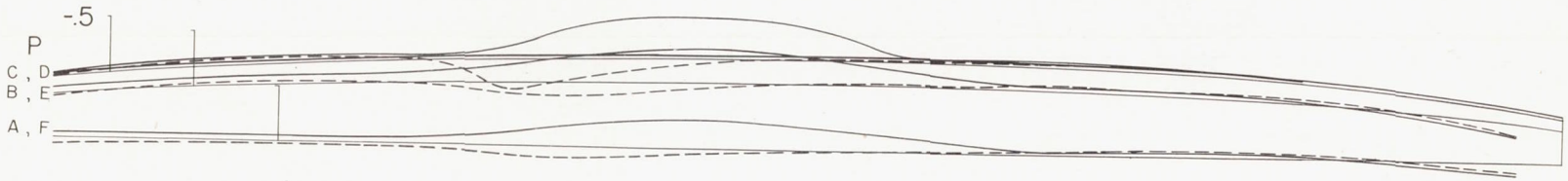

M = 0.80.

Figure 5.- Pressure distributions and tuft patterns. $\alpha = 6^{\circ}$.

L-74408

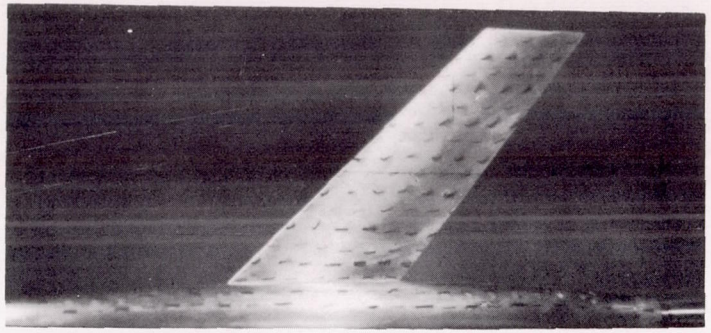

M = 0.79

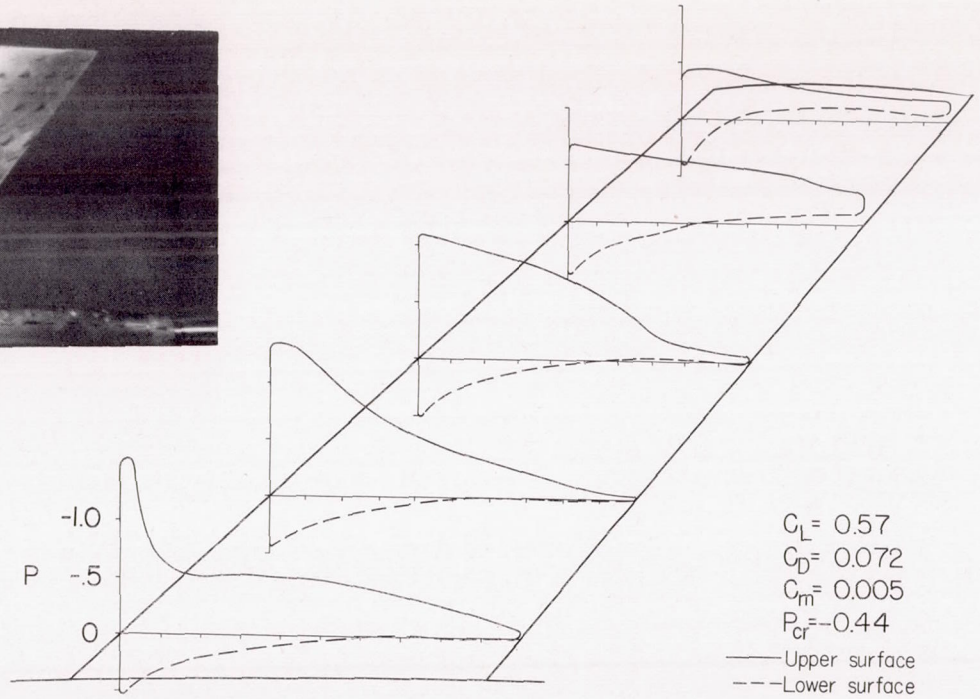

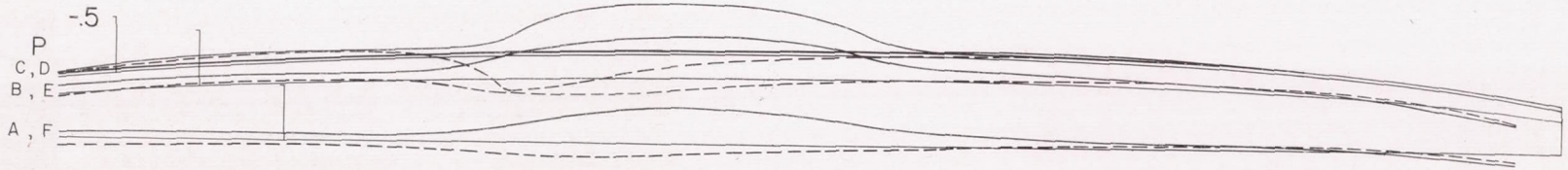

(a) M = 0.80.

Figure 6.- Pressure distributions, tuft patterns, and schlieren surveys. $\alpha = 8^{\circ}$.

NACA

L-74409

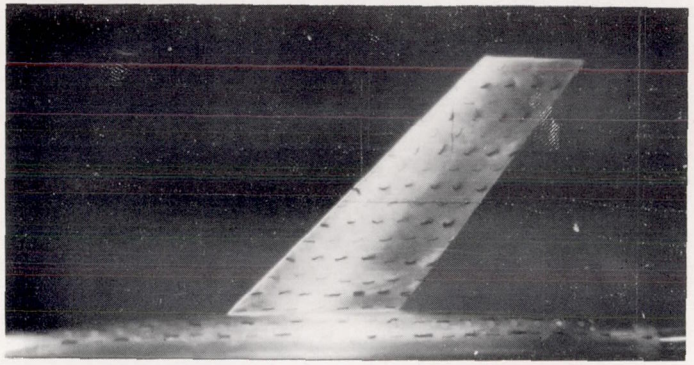

M = 0.84

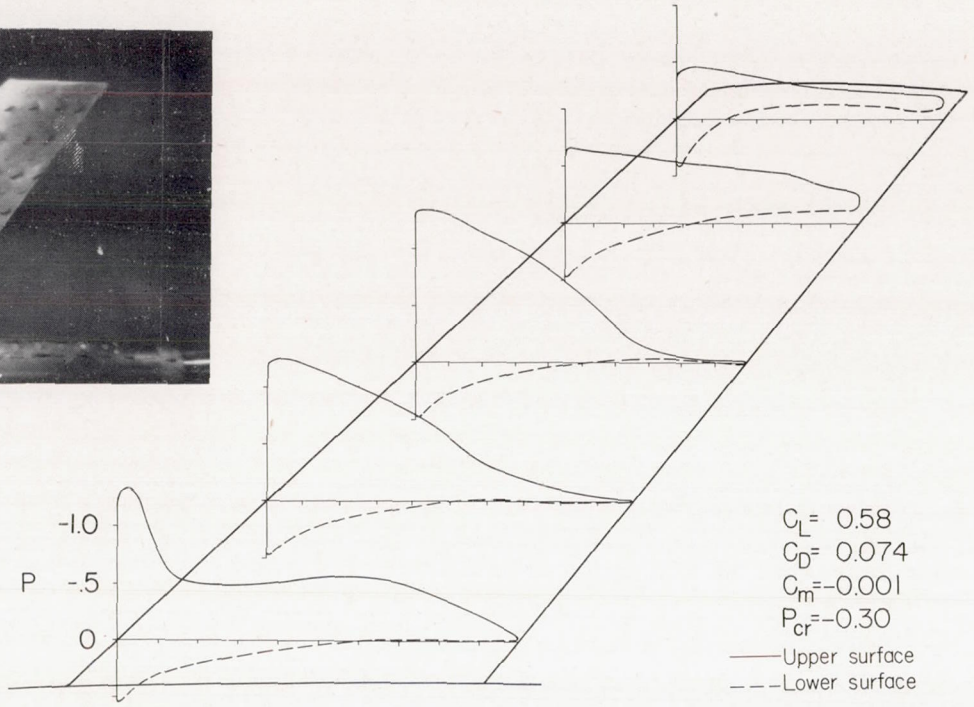

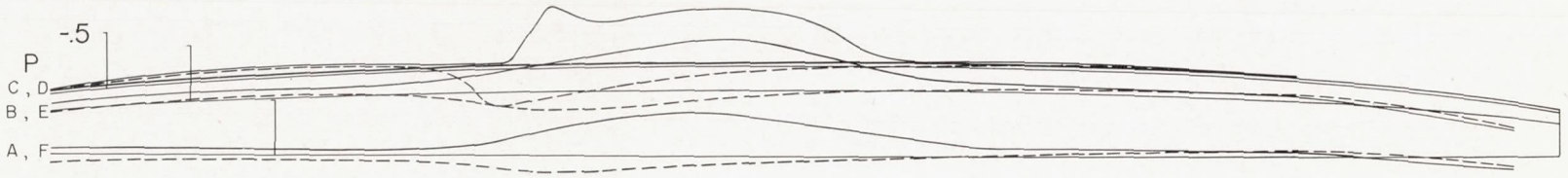

(b) M = 0.85.

Figure 6.- Continued.

NACA

L-74410

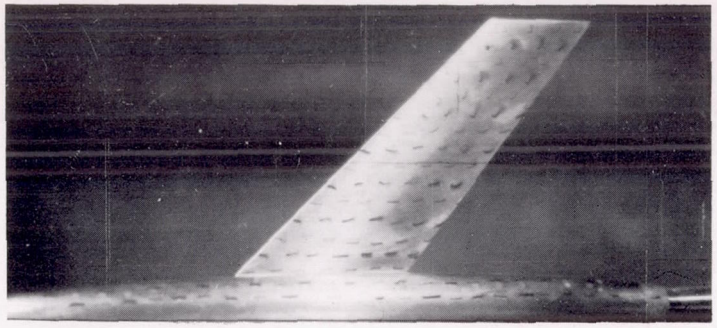

M = 0.89

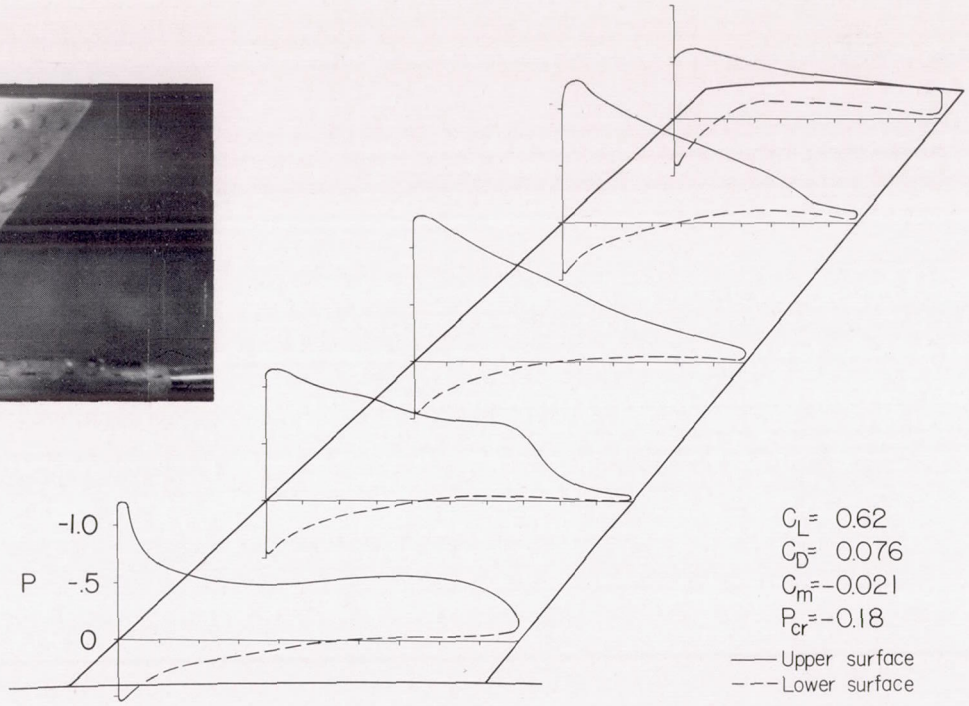

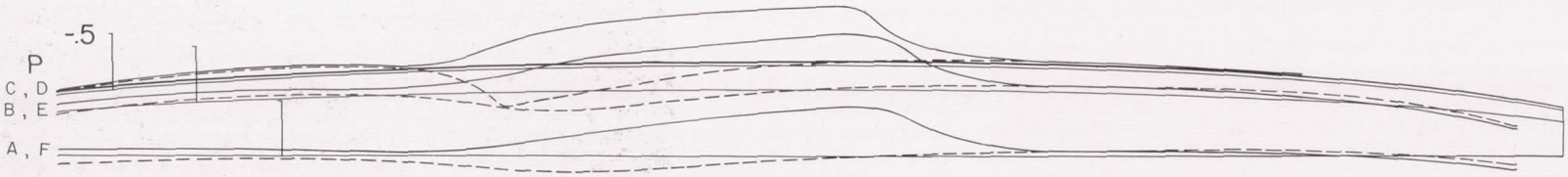

(c) M = 0.90.

Figure 6.- Continued.

NACA

L-74411

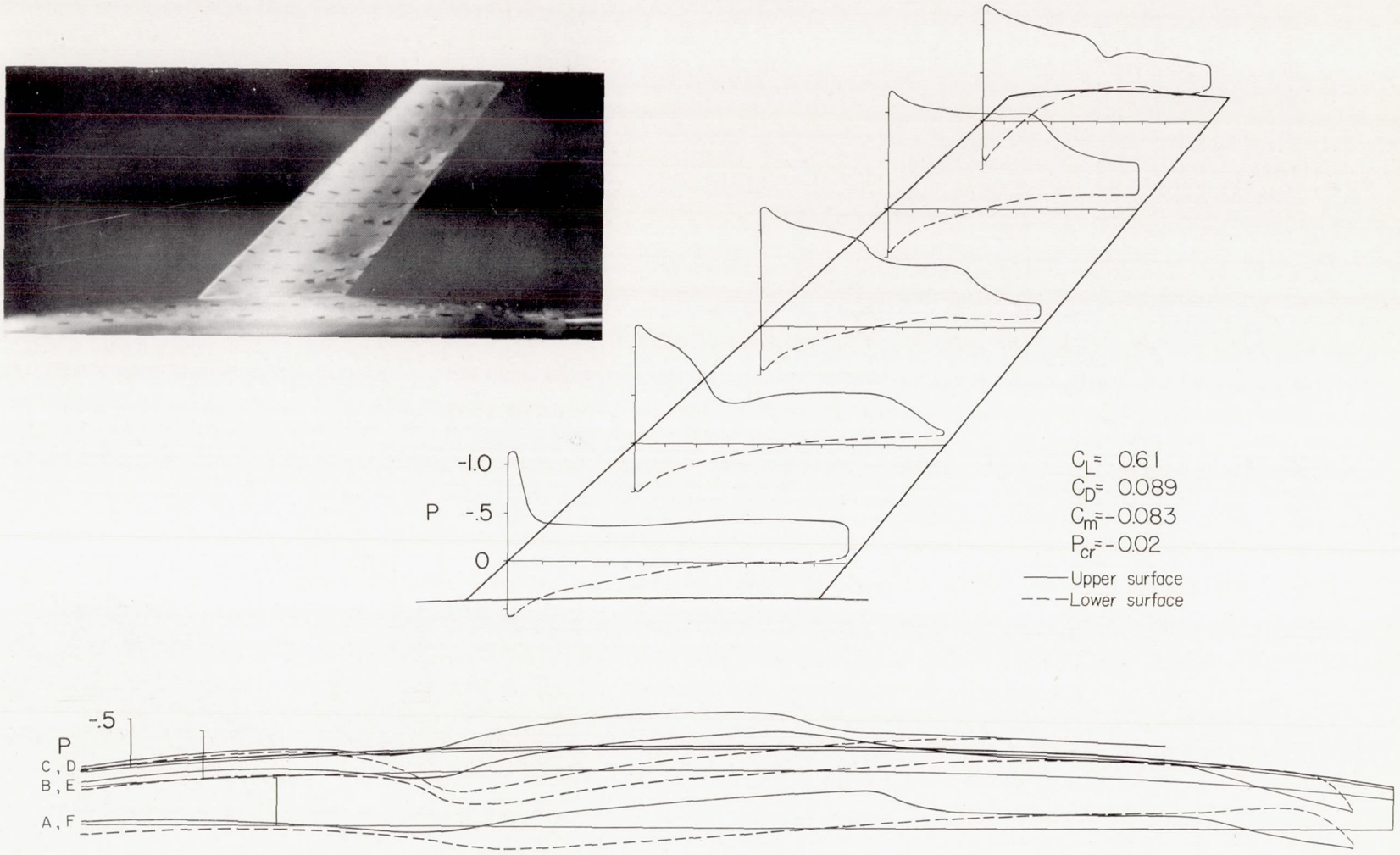

(d) M = 0.99.

Figure 6.- Continued.

NACA

L-74412

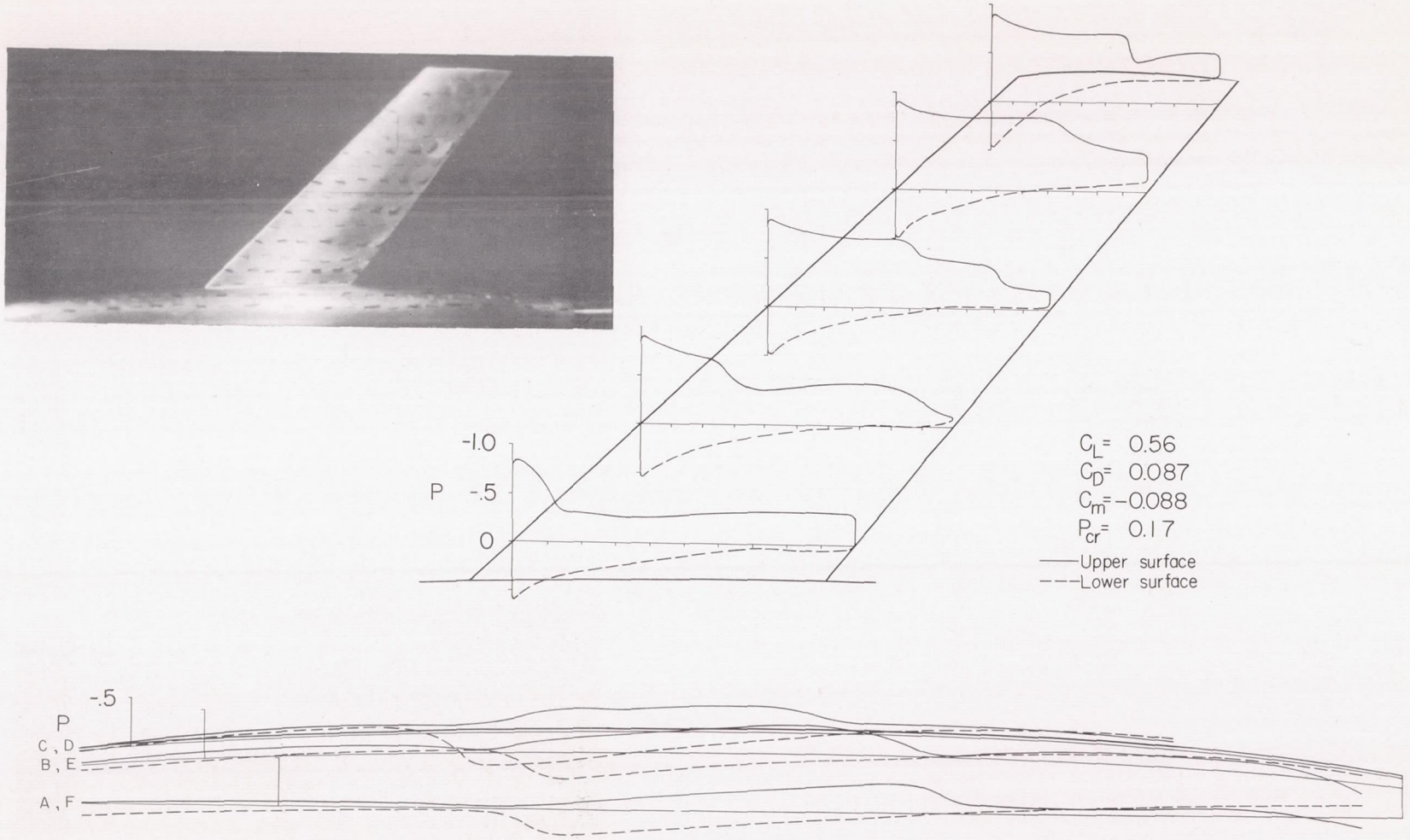

(e) M = 1.11.

Figure 6.- Concluded.

NACA

L-74413

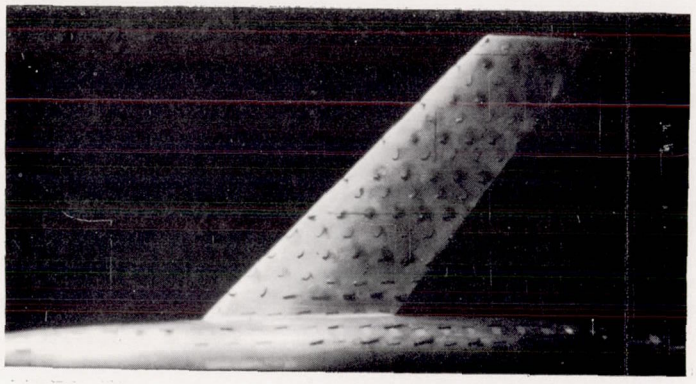

M = 0.79

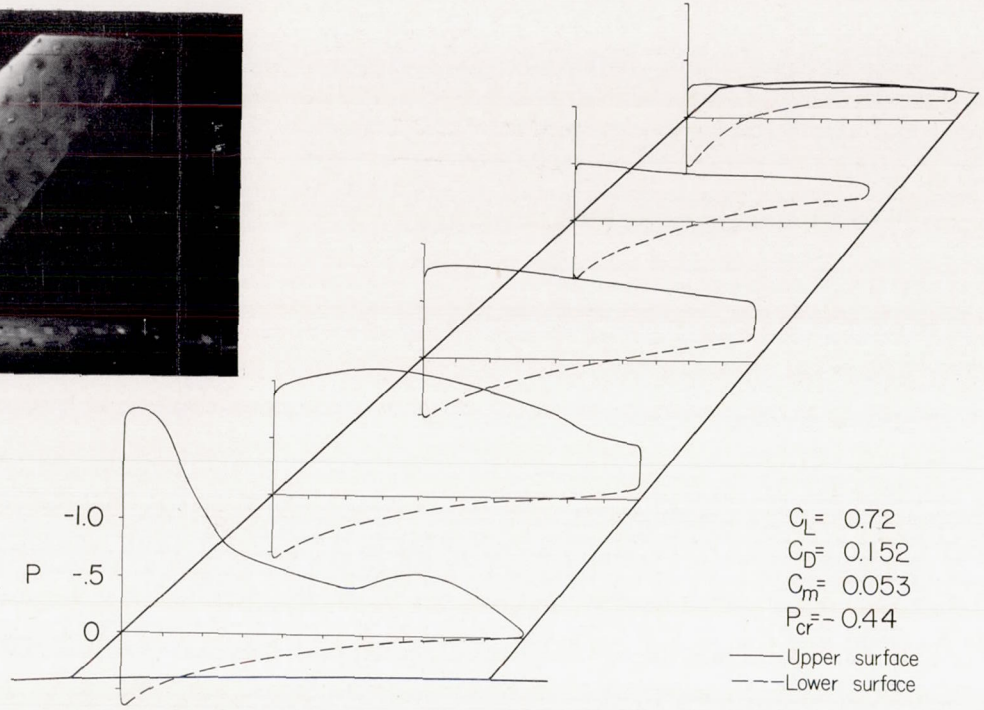

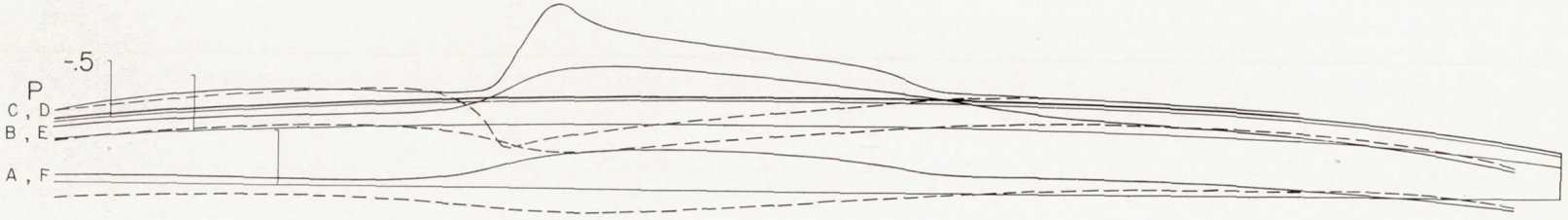

(a) M = 0.80.

Figure 7.- Pressure distributions and tuft patterns. $\alpha = 12^{\circ}$.

L-74414

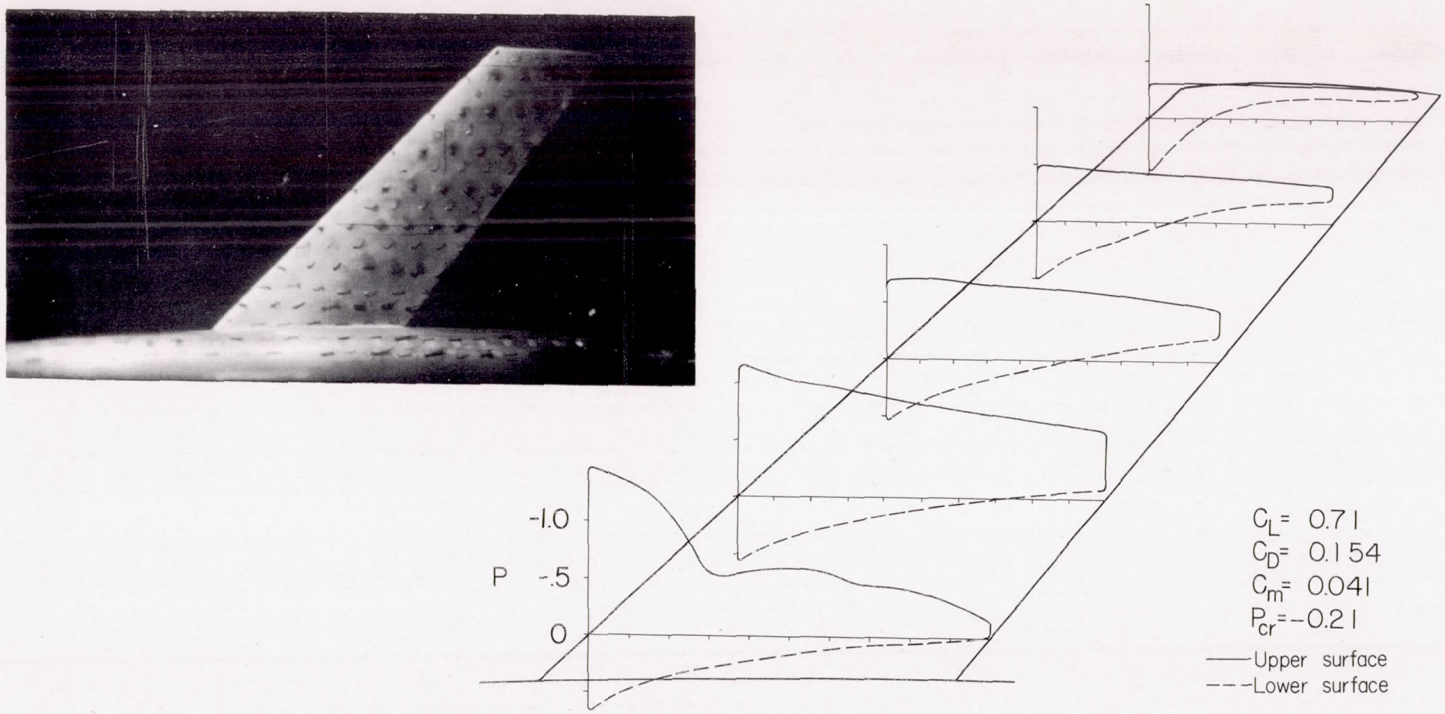

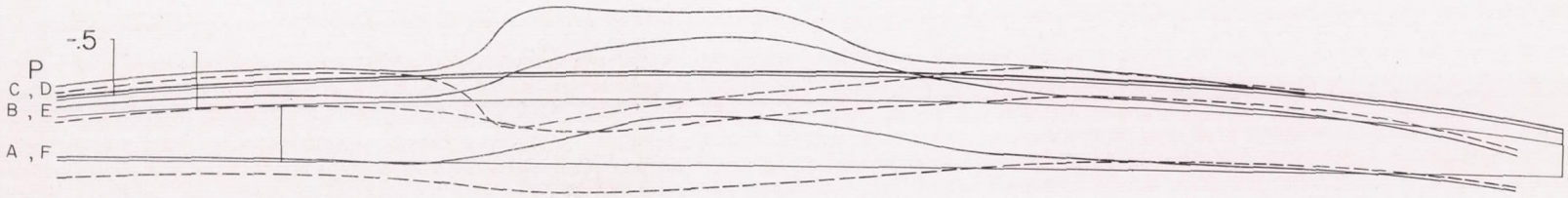

(b) M = 0.89.

Figure 7.- Continued.

NACA

L-74415

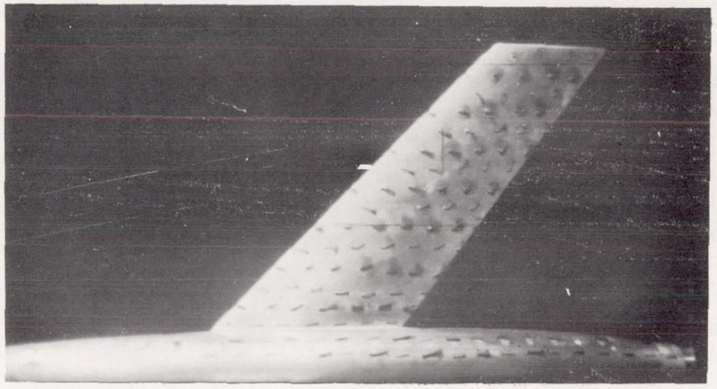

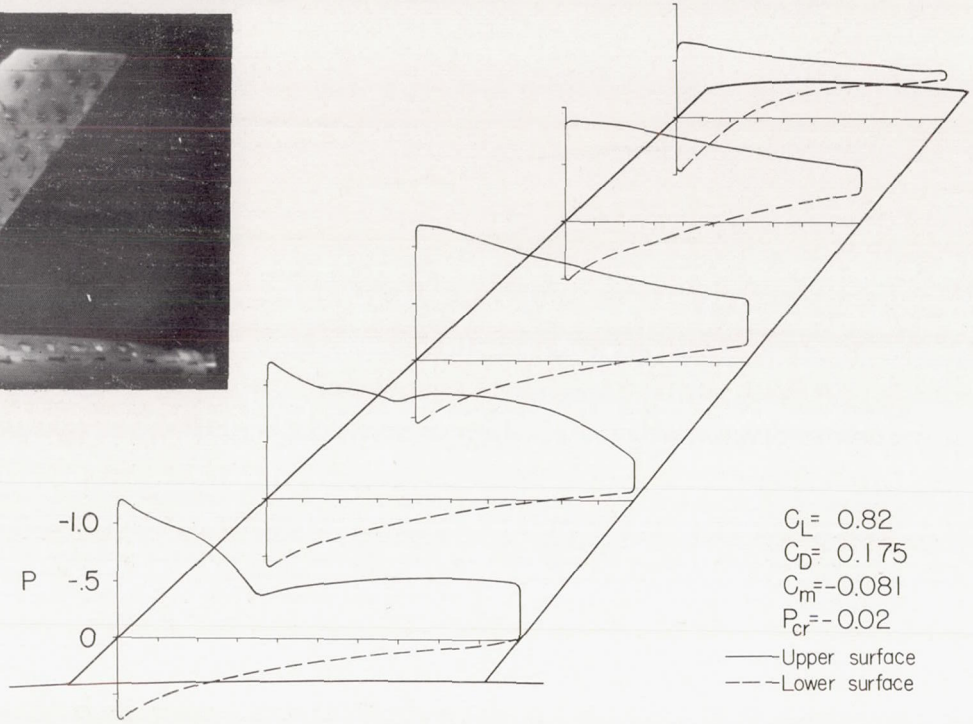

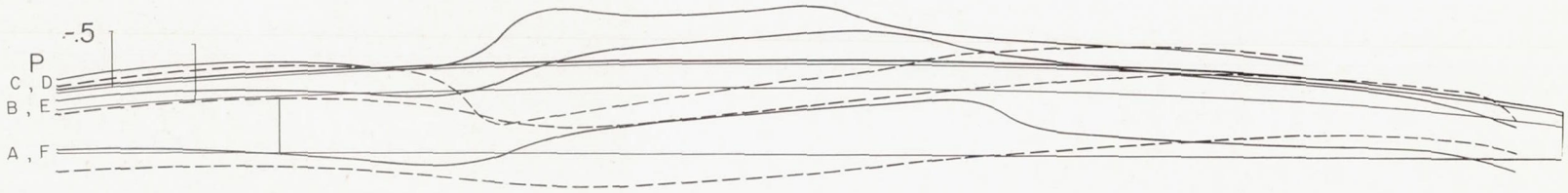

(c) M = 0.99.

Figure 7.- Continued.

NACA

L-74416

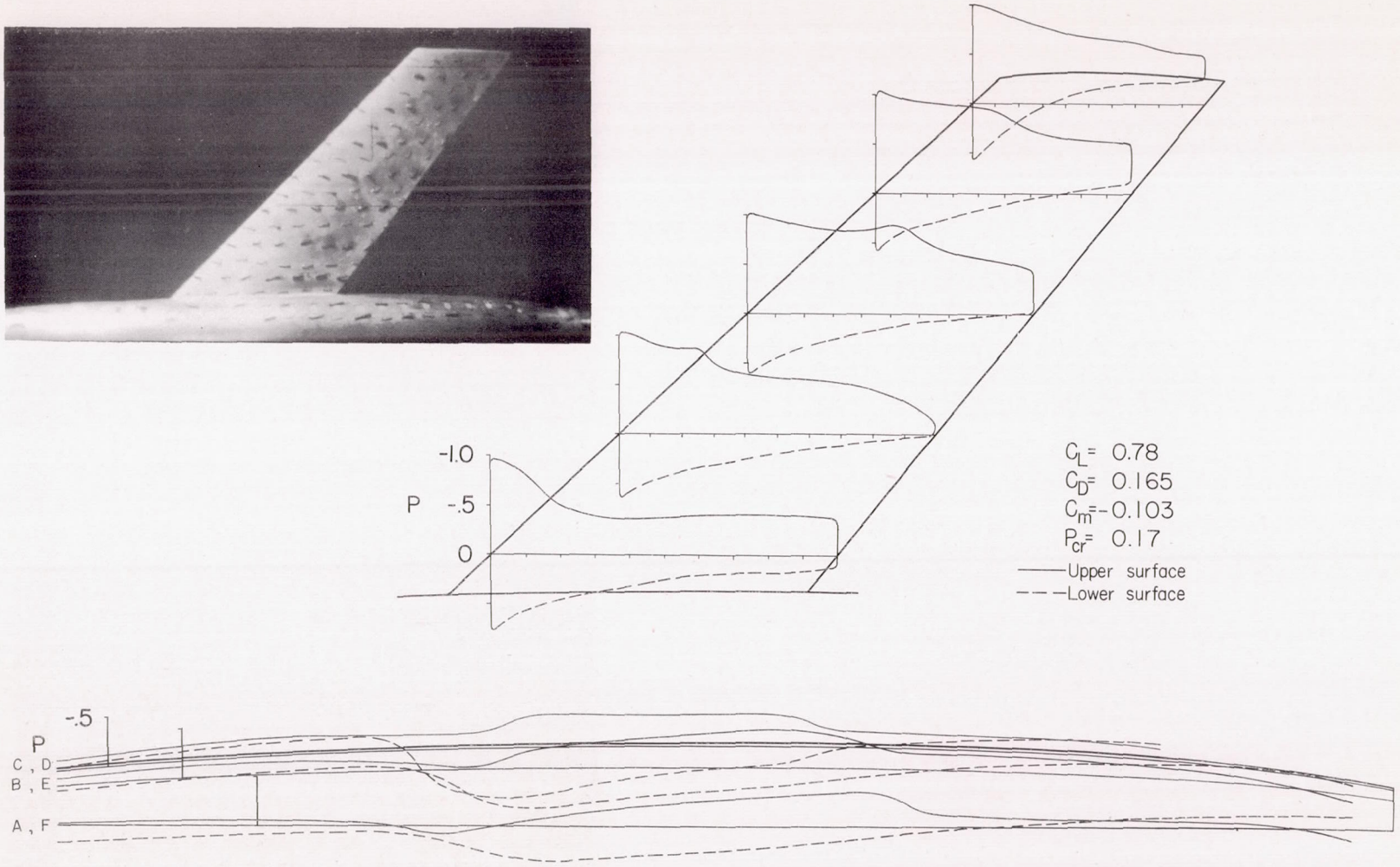

(d) M = 1.11.

NACA

L-74417

Figure 7.- Concluded.

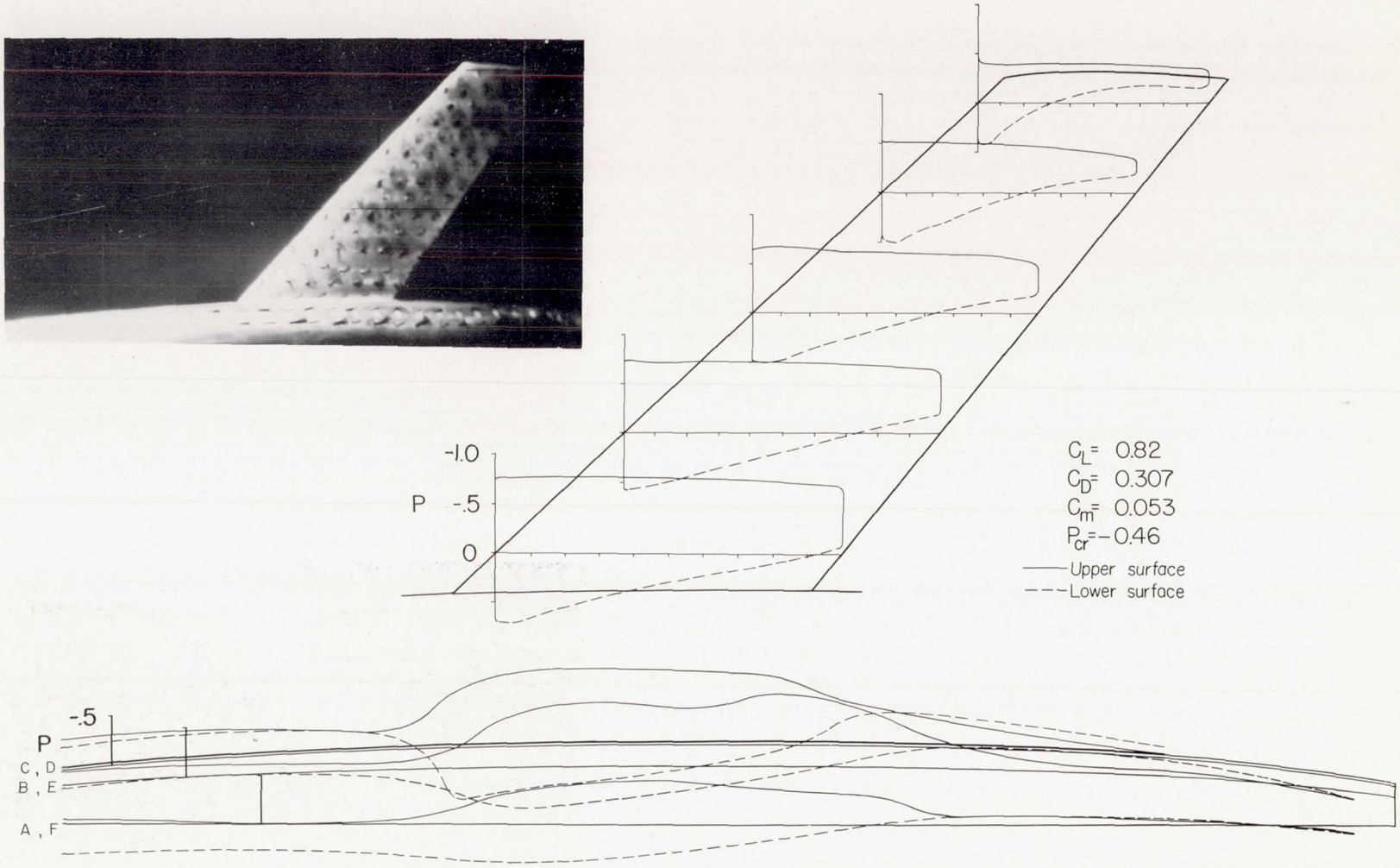

(a) M = 0.79.

Figure 8.- Pressure distributions and tuft patterns. $\alpha = 20^{\circ}$.

L-74418

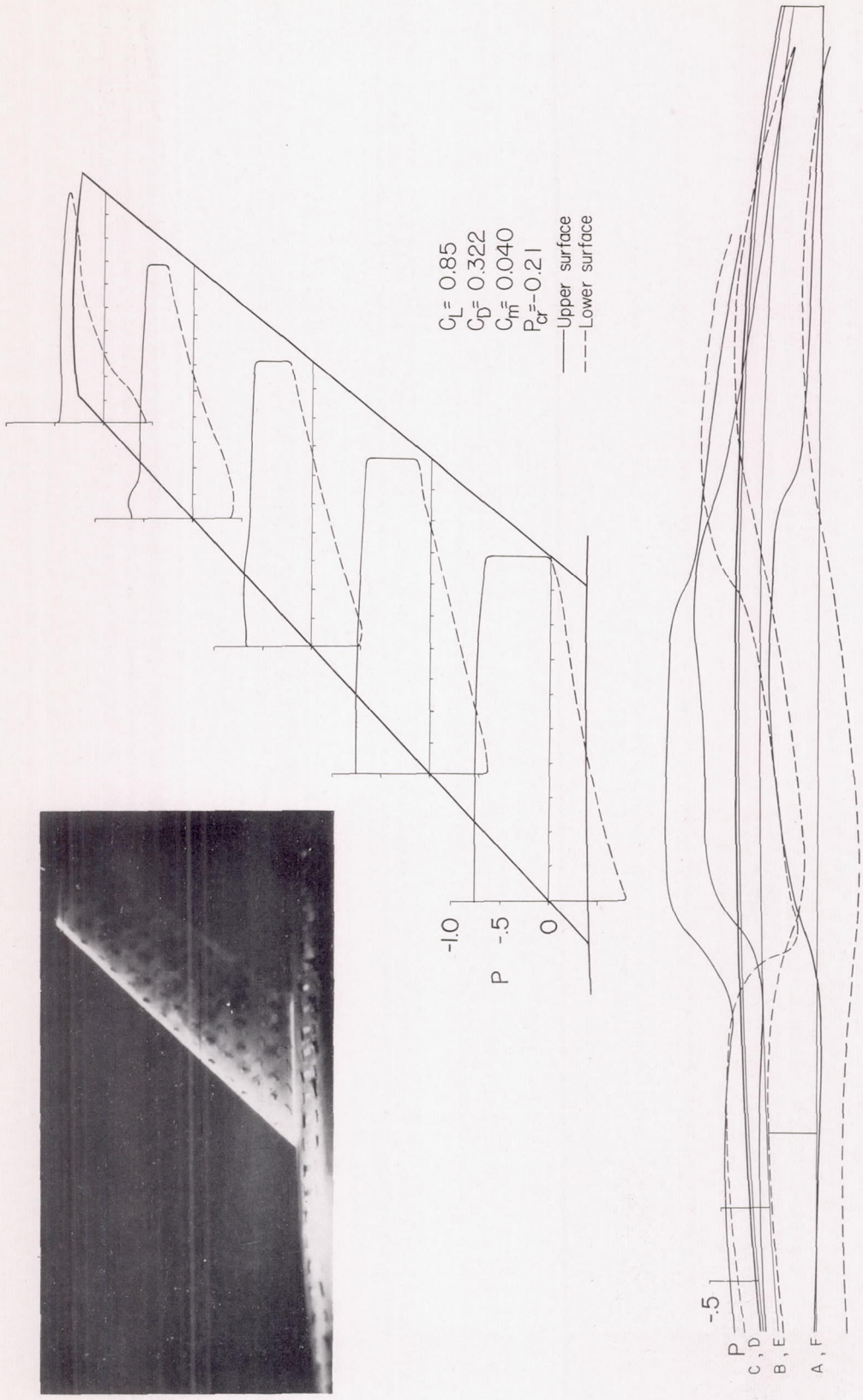

(b) M = 0.89.

Figure 8.- Continued.

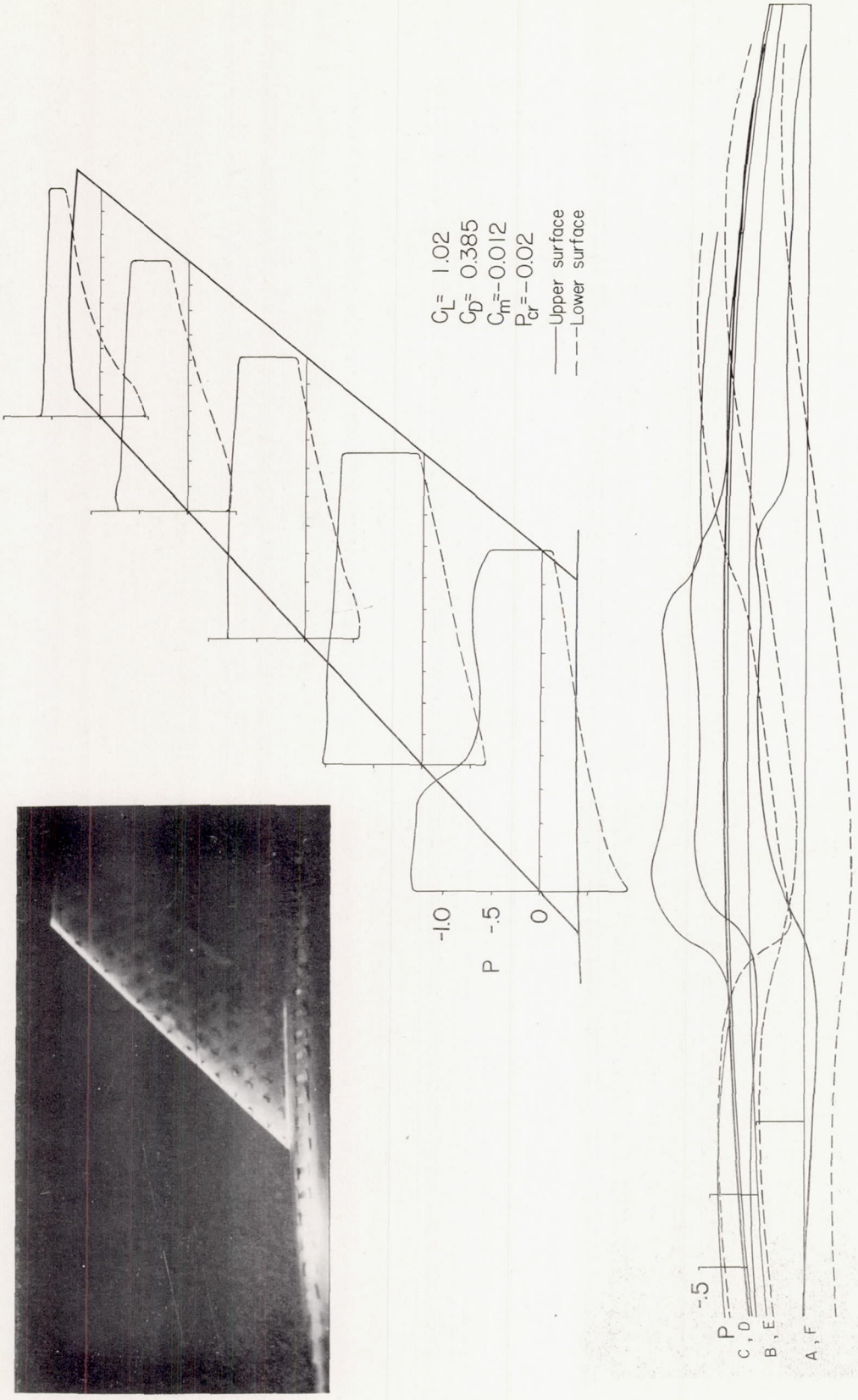

(c) M = 0.99.

Figure 8.- Continued.

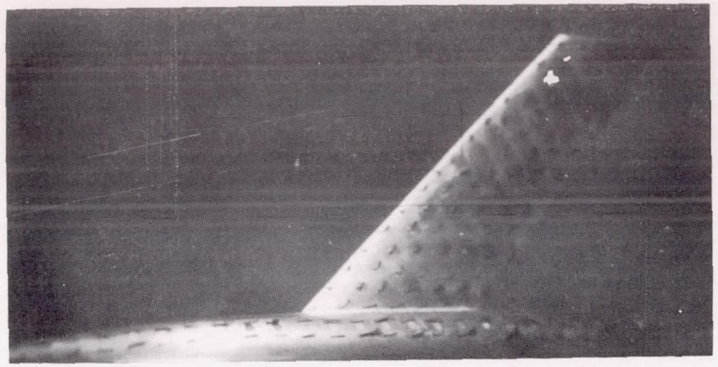

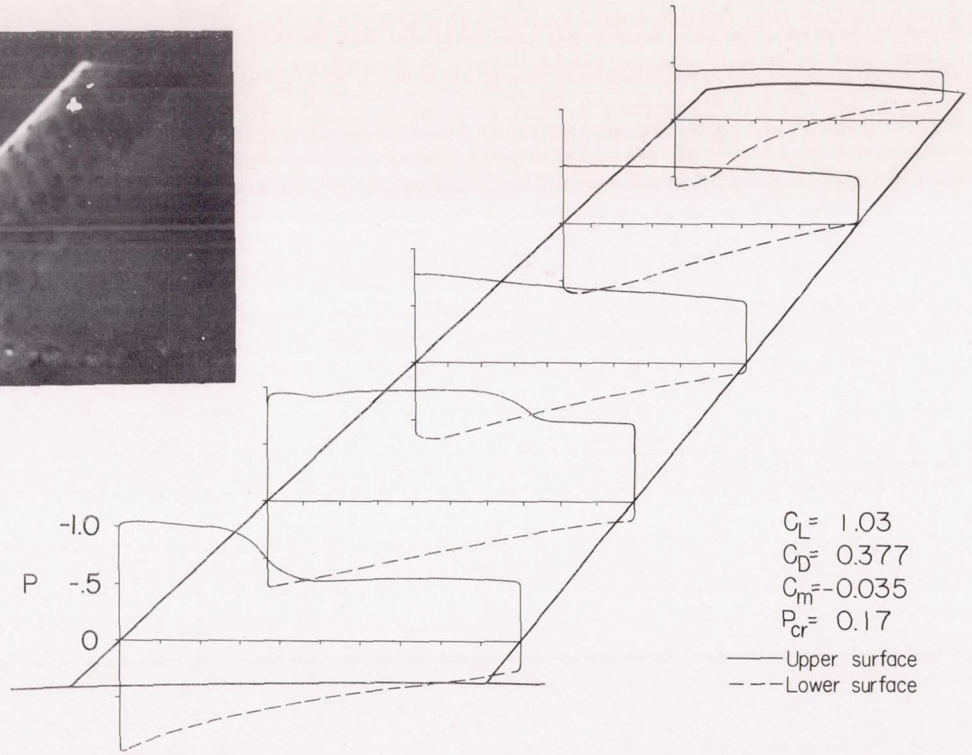

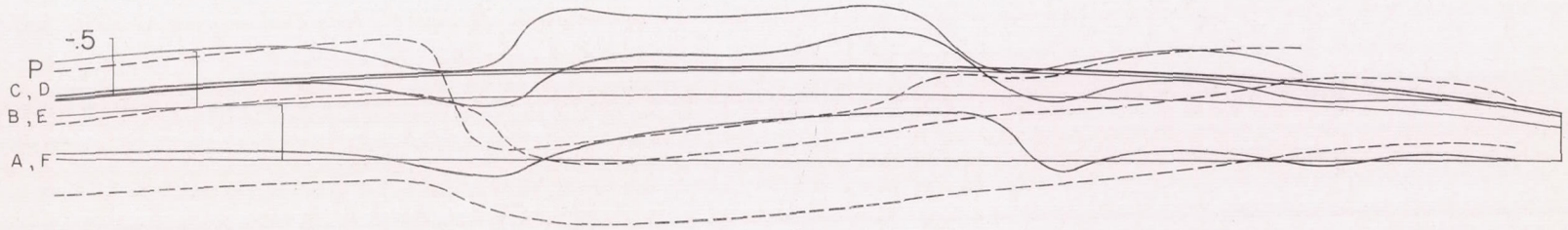

(d) M = 1.11.

Figure 8.- Concluded.

NACA

L-74421

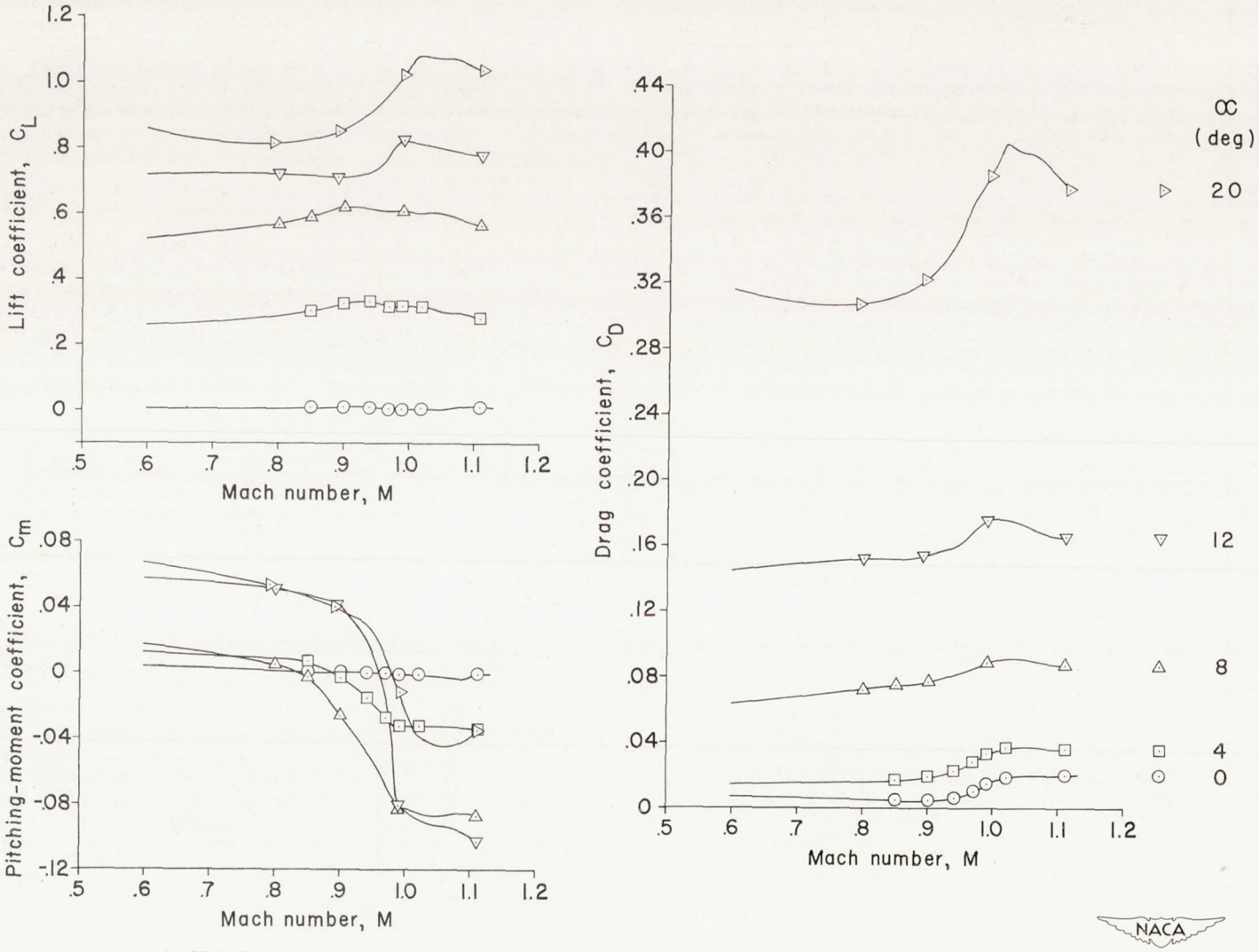

Figure 9.- Variation with Mach number of the force and moment characteristics for the wing-fuselage combination.